mRNA expression and immunocytochemical localization of galectin-1 in IMS32 cells

IMS32 cells showed distinct Schwann cell phenotypes, such as spindle shaped morphology under phase contrast microscopy (Fig. 5A) and intense immunoreactivity for S100, p75 low affinity NGF receptors, laminin and several Schwann cell-specific transcription factors and neurotrophic factors (Watabe *et al.*, 1995, 2003). By Northern blot analysis with an alkaline phosphatase-labelled cDNA probe, galectin-1 mRNA was detected as a single band corresponding to the molecular weight of ≈0.6 kilobase pairs (kb) (Fig. 5B). This result suggests biosynthesis of galectin-1 in IMS32 cells. Immunocytochemistry with antigalectin-1 antibody revealed the intense immunoreactivity not only in the cytoplasm of IMS32 cells but also on the cell surface and/or in the extracellular space with vesicular shapes (Fig. 5C). This immunohistochemical appearance was more prominent than that in adult rat Schwann cells (Fig. 3F), and is consistent with previous findings with different kinds of cells (Cooper & Barondes, 1990; Avellana-Adalid *et al.*, 1994; Cho & Cummings, 1995; Lutomski *et al.*, 1997).

Electron microscopy for intracellular and extracellular detection of galectin-1

Electron microscopic studies with immunocytochemistry revealed that the immnogold labelling was found mainly at the periphery and/or outside the soma of DRG cells (Fig. 6A) and IMS32 cells (Fig. 6B). Substitution of the primary antibody with preimmune rabbit IgG resulted in no staining (Fig. 6C). The intracellular electron-dense materials (indicated as asterisks in Fig. 6A and C) appear to be lysosomes.

Detection of galectin-1 in the culture medium of DRG neurons and IMS32 cells

The findings from immunocytochemistry (Figs 3–6) suggested that galectin-1 was externalized from DRG cells (neurons and Schwann cells) and IMS32 cells to culture media. To confirm this, we collected the conditioned media from these cells and analysed them by Western blots using antigalectin-1 antibody. As shown in our previous study (Inagaki *et al.*, 2000), the average molecular mass of recombinant human galectin-1 purified from COS1 cells (oxidized form, Fig. 7, lane 4) was slightly smaller than that of the reduced form of the protein (Fig. 7, lane 1). Under the condition without a reducing agent, both reduced and oxidized forms of galectin-1 were detected in culture medium of IMS32 (Fig. 7, upper panel, lane 3) and DRG neurons (Fig. 7, lower panel, lane 3).

Very few trypan-blue-positive IMS32 cells were observed (< 0.1% of the cells at any observation area) at 48 h after seeding (not shown), suggesting that cell death was so low that it could not have contributed to galectin-1 in the conditioned medium. Although galectins are water-soluble proteins, it is necessary for the purification of cytosolic galectins to add some hapten sugars such as lactose to an extraction buffer (Kasai & Hirabayashi, 1996). This means that the lectin molecules can hardly be dissociated from water-insoluble substances of cells without the hapten sugars, when cells are damaged or lysed. The serum-free culture medium used for the release experiments in this study did not contain lactose or other galactose-containing saccharides. Supposing cell death and lysis occurred during the culture in the medium, it would be hardly possible for galectin-1 or other galectins to be separated from water-insoluble materials of dead cells and move from the cytosol to the culture supernatants. Therefore, most galectin-1 molecules in the culture supernatants detected by Western blotting are likely to be those which were externalized from viable cells.

Discussion

Many studies have suggested that galectins are involved in cell–cell and cell–matrix interactions during neural development (Puche *et al.*, 1996; Pesheva *et al.*, 1998) and progression and migration of brain tumours (Camby *et al.*, 2001; Lahm *et al.*, 2001). However, much less attention has been paid to the functional significance of the molecules in mature nervous tissues. In the present study, we focused on mRNA expression, immunochemical localization, and externalization of galectin-1 in mature DRG and peripheral nerves. *In situ* hybridization and immunohistochemistry (Figs 2 and 3A) revealed an intense expression of galectin-1 in DRG neurons with smaller diameters, which was in agreement with previous findings (Regan *et al.*, 1986; Hynes *et al.*, 1990). There may be a discrepancy between the findings from *in situ* hybridization and those from immunohistochemistry: mRNA expression, but not immunoreactivity for galectin-1, was detected in larger neurons. The immunohistochemistry on DRG sections (Fig. 3A) was carried out with antigalectin-1 antibody, which was diluted to 1 : 1000 with 0.5% skimmed milk. However, the immunohistochemistry with higher concentration of the antibody (1 : 200–1 : 300) resulted in weak but visible immunoreactivity for galectin-1 in larger neurons (K. Sango and K. Ajiki, unpublished observations). This result was consistent with that of our previous study (Fukaya *et al.*, 2003), in which the antibody was diluted 1 : 100 prior to use. Taking these findings into consideration, galectin-1 is likely to be synthesized in and distributed to all DRG neurons. Also, it is obvious from those studies that both mRNA expression and immunoreactivity for this lectin in smaller neurons are much more intense than those in larger neurons in intact DRG. The small neurons were reported to have small axonal fibres such as Aδ and C, which can play an essential role in mechanical and polymodal nociception (Salt & Hill, 1983). Therefore, cytosolic galectin-1 in small DRG neurons may be involved in such small-fibre functions. A recent study by Senba *et al.* (2001) revealed that most of galectin-1-immunoreactive DRG neurons expressed mRNA for c-ret but not for trkA. Because c-ret and trkA are proto-oncogenes of the functional receptors for glial cell line-derived neurotrophic factor (GDNF) and nerve growth factor (NGF), respectively (Kashiba *et al.*, 1998), this finding suggests that galectin-1 is expressed in GDNF-responsive DRG neurons rather than NGF-responsive neurons. Regan *et al.* (1986) observed intense immunoreactivity for galectin-1 in the central processes of DRG neurons (i.e. dorsal funiculus and dorsal horn) in embryonic and neonatal rats, but the immunoreactivity was decreased and restricted to the superficial dorsal horn in adult rats. In contrast, Senba *et al.* (2001) showed axotomy-induced up-regulation of galectin-1 in the dorsal horn of adult rats, suggesting a role for endogenous galectin-1 in the pathological pain due to nerve injury. By RT-PCR analysis (Fig. 1), galectin-1 mRNA was detected in both ganglia and spinal nerve fibres. Because the latter do not contain neuronal cell bodies, this finding suggests that galectin-1 can be synthesized in non-neuronal cells of nerve fibres. Although it was difficult to conclude the expression of galectin-1 mRNA in non-neuronal cells by *in situ* hybridization (Fig. 2), immunohistochemistry showed that Schwann cells within the spinal nerve sections were intensely stained with the galectin-1 antibody (Fig. 3A). This is consistent with previous findings using sections of rat sciatic nerves (Fukaya *et al.*, 2003). Taking the results of RT-PCR and immunohistochemistry together, it appears likely that galectin-1 is synthesized in Schwann cells. Consistently, Northern blot analysis (Fig. 5B) showed galectin-1 mRNA expression in the spontaneously immortalized adult mouse Schwann cells (IMS32).

In contrast to the studies *in vivo*, galectin-1 immunoreactivity was observed in almost all DRG neurons from a very early stage (3 h) in

B

kb

6.6→

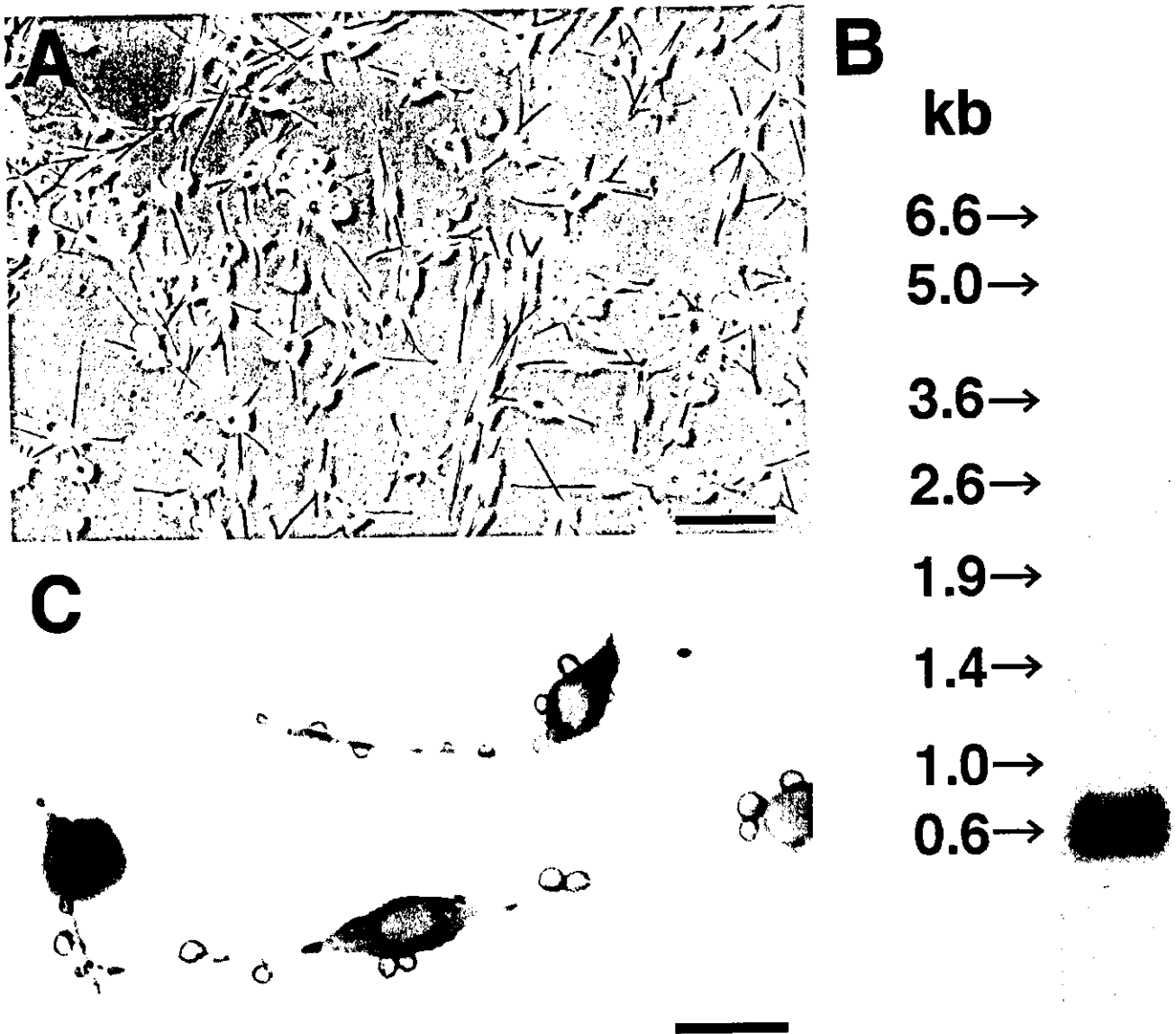5.0→

3.6→

2.6→

1.9→

1.4→

1.0→

0.6→

C

FIG. 5. Expression of galectin-1 in immortalized adult mouse Schwann cells (IMS32). (A) A phase-contrast micrograph of IMS32 cells. (B) Northern blot analysis of IMS32 cell mRNAs. After transfer, the bound mRNAs were hybridized with a 408-bp rat galectin-1 cDNA probe labelled with AlkPhos Direct (Amersham Biosciences). Marker molecular masses for calibration are indicated on the left. (C) Immunocytochemical localization of galectin-1 in IMS32 cells. Intense immunoreaction with vesicular shapes was observed on the cell surface protruding to an extracellular space, suggesting the externalization of galectin-1 from the cells. Scale bars, 50 μm (A), 10 μm (C).

culture (Fig. 3B). Enzymatic and mechanical treatments for the dissociation of DRG cells, together with disruption of the interactions between neurons and satellite cells, are detrimental to the survival of neurons, and some neurons die during in vivo–in vitro replacement (Sango et al., 1991, 2003; Kasper et al., 1999). Therefore, galectin-1 expressed in cultured DRG neurons may play a role in the repair of neurons from injury caused by the dissociation procedure and/or protection of neurons from death at the initial phase in culture. As the culture time increased, galectin-1 immunoreactivity became concentrated at the surface of neurons (Fig. 3C–E). In addition, Schwann cells proliferated and began to express galectin-1 at later stages in culture (Fig. 3E). At a higher magnification, the immunoreactivity for galectin-1 was visualized as vesicles budding off the surface of Schwann cells (Fig. 3F). These light microscopic findings were consistent with the results of immunoelectron microscopy (Fig. 6) and indicate the extracellular release of galectin-1 from neurons and

Schwann cells in culture. This was further confirmed by Western blot analysis: both reduced and oxidized forms of galectin-1 were detected in the culture media of DRG neurons (Fig. 7, lower panel) and IMS32 cells (Fig. 7, upper panel) under nonreducing conditions. The immunoreactivity for galectin-1 in the medium of DRG neurons was much lower than that in the medium of IMS32 cells, which may be because the culture medium was initially collected at 48 h after seeding. Immunocytochemical studies showed localization of galectin-1 on the surface of DRG neurons beyond 2 days in culture, suggesting that the extracellular release of this molecule may be increased at later stages of culture. In contrast, the surface and extracellular immunoreactivities for galectin-1 were observed in IMS32 cells at all observation periods, from 1 to 4 days after seeding. Thus, it appears that IMS32 cells constantly synthesize and secrete galectin-1 regardless of incubation time. IMS32 cells have been established from long-term cultures of adult mouse DRG and peripheral nerves (Watabe et al., 1995).
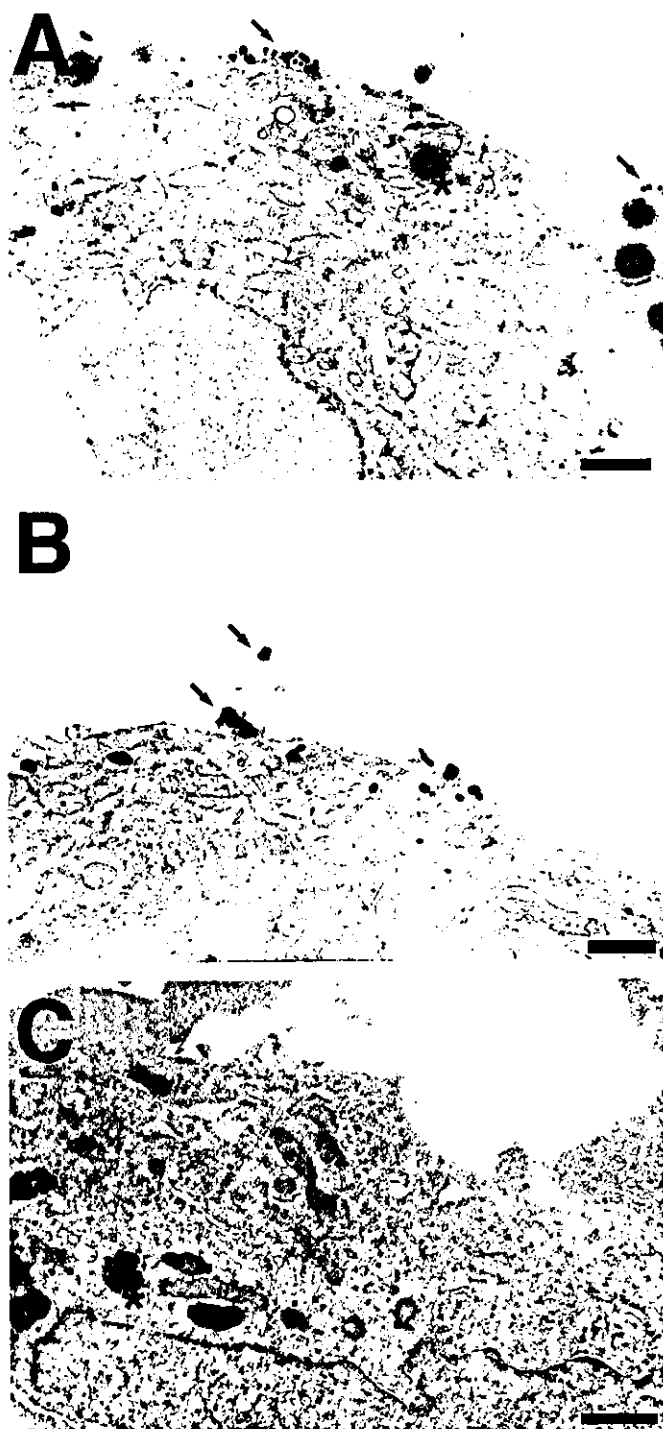
FIG. 6. Electron micrographs of (A) adult rat DRG neurons and (B) IMS32 cells, stained with an antibody to galectin-1. Cells at 7 days after seeding were processed for immunocytochemistry and embedded in epoxy resin. The immunogold particles (indicated as arrows in A and B) were found mainly at the cell periphery and/or outside the cell soma. (C) Substitution of the primary antibody with preimmune rabbit IgG resulted in no staining. The intracellular electron dense materials (indicated as asterisks in A and C) appeared to be lysosomes. cale bars, 1 μm (A), 0.5 μm (B), 0.7 μm (C).

These cells showed distinct Schwann cell phenotypes as described in Results, as well as in previous reports (Watabe *et al.*, 1995, 2003). Although IMS32 cells are different from primary and long-term cultured Schwann cells in that the former were not contact-inhibited
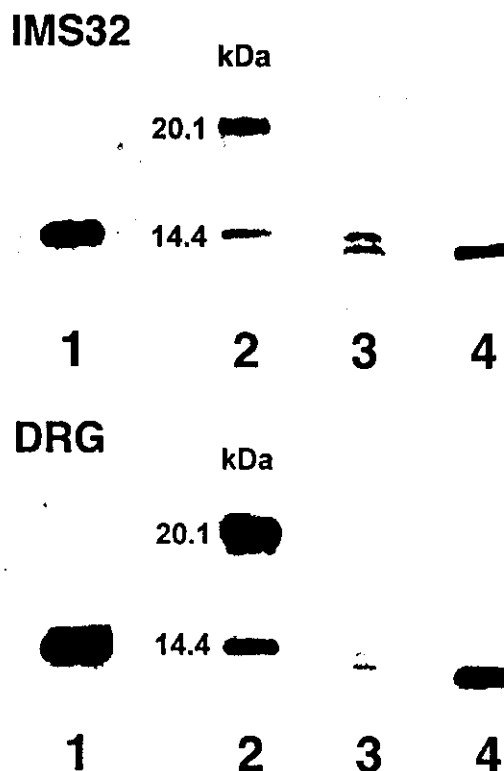

FIG. 7. Western blot analysis of culture medium obtained from IMS32 cells (upper panel) and DRG neurons (lower panel) for galectin-1. Oxidized recombinant human galectin-1 (2 ng) (lanes 1 and 4) and the culture supernatant of IMS32 cells (lane 3, upper panel) and DRG neurons (lane 3, lower panel) were analysed by SDS–PAGE on a 15–25% gradient gel in the presence (lane 1) or absence (lanes 3 and 4) of 20 mM dithiothreitol. Immunocomplexes on the blotted membrane were visualized by chemiluminesence using an image analyser. Molecular size markers are shown in lane 2.

and formed ball-shaped subcolonies when cultures reached confluence, IMS32 cells exhibit mitogenic responses to several growth factors [e.g. platelet-derived growth factor (PDGF)-BB, acidic and basic fibroblast growth factor (aFGF, bFGF), transforming growth factor (TGF)-β1,2] which were similar to primary and long-term cultured Schwann cells (Watabe *et al.*, 1994). Immunocytochemistry on IMS32 cells and primary-cultured Schwann cells which were kept in the same culture media (i.e. DMEM or F12 in the presence or absence of serum) revealed that the former showed more intense cytosolic immunoreactivity for galectin-1 with more extensive vesicle formation outside the cell soma than did the latter, under any culture conditions (not shown). These findings imply that IMS32 cells could produce and externalize higher amounts of galectin-1 than primary-cultured Schwann cells, regardless of components of the culture medium. The detection of both reduced and oxidized forms of galectin-1 suggested that some galectin-1 molecules externalized from DRG neurons or IMS32 cells were oxidized. The physiological extracellular environment appears to be oxidative, and injury-induced nitric oxide (NO) in the extracellular space may accelerate the oxidization of galectin-1 (Guizar-Sahagun *et al.*, 1998). However, it remains possible that oxidization of the molecule takes place during electrophoresis without a reducing agent. We are currently trying to develop a monoclonal antibody which could specifically recognize the oxidized form of galectin-1. Such an antibody would be helpful in obtaining more precise information about the form of galectin-1 on the cell surface and in the extracellular space.

Galectin-1 is not a typical secreted protein because cDNA sequences of galectin-1 lack a recognizable secretion signal (Clerch *et al.*, 1988; Wilson *et al.*, 1989). Based on the findings from immunocytochemical studies with myogenic cells, Cooper & Barondes (1990) hypothesized a 'nonclassical' pathway for its secretion as follows. Galectin-1, initially distributed throughout the cytosol, becomes concentrated in the cytoplasm beneath the plasma membrane (ectoplasm), accumulates in restricted regions of ectoplasm and evaginates to form extracellular vesicles. Subsequent disruption of the evaginated vesicles results in a release of the lectin into the extracellular milieu. This hypothesis is supported by findings from previous studies which used several cell lines (Avellana-Adalid *et al.*, 1994; Cho & Cummings, 1995; Lutomski *et al.*, 1997) and the present study with DRG neurons and Schwann cells. The externalization of galectin-1 accompanies differentiation of myoblasts (Cooper & Barondes, 1990) and leukaemia cell lines (Lutomski *et al.*, 1997), whereas induction of neuroblastoma differentiation markedly decreased its externalization (Avellana-Adalid *et al.*, 1994). These findings imply that galectin-1 secretion is tightly controlled during development and differentiation (Hughes, 1999). In contrast, the results in the present study suggest its release from DRG neurons and Schwann cells of adult animals in culture. Because some biological properties of these cells change with postnatal development and maturation (Lindsay, 1988; Horie *et al.*, 1990; Chi *et al.*, 1993), it appears that the culture system of adult DRG is useful for the study of plasticity and regeneration of the peripheral nervous system (Sango *et al.*, 2003). The nonclassical pathway for the secretion of galectin-1 shown in neurons and Schwann cells *in vitro* may be, at least partially, applicable to these cells *in vivo*. In fact, intense immunoreactivity for galectin-1 was observed in the axons and Schwann cells which had regenerated or migrated into a grafted silicone tube after transection of adult rat peroneal nerves (Horie *et al.*, 1999). Therefore, cytosolic galectin-1 is likely to be released from growing axons and Schwann cells into the extracellular space upon axonal injury. Galectin-1 is distributed to both neuronal cell bodies and axons in intact peripheral nerves (Horie *et al.*, 1999; Fukaya *et al.*, 2003), suggesting that the lectin molecules synthesized in the cell soma are transported to the axon terminals (Kitchener *et al.*, 1994). However, it should be noted that in this study the immunoreactivity for galectin-1 was localized at the cell soma, not at the neurites of DRG neurons in culture in the absence of serum (Fig. 4A–C). In contrast, the intense immunoreactivity was detected in both neuronal cell bodies and neurites in culture in the presence of serum (Fig. 4D–F). The latter finding is consistent with that *in vivo* and suggests galectin-1 transport from the neuronal cell bodies to the neurites. It is recognized that neurons kept in serum-containing medium could survive and extend neurites better than those kept in serum-free medium (Oorschot & Jones, 1986; Sango *et al.*, 1991; Sotelo *et al.*, 1991). This suggests that survival and neurite formation of cultured neurons could be promoted by known and unknown factors contained in serum. Similarly, it appears that some molecules in serum could facilitate synthesis and/or axonal transport of galectin-1 in DRG neurons. On the other hand, most of the cultures were kept in serum-free medium in this study in order to avoid the effects of serum-derived factors on the extracellular expressions of galectin-1.

It is possible that galectin-1 released from neurons and Schwann cells acts on peripheral nervous tissues in an autocrine fashion. Many studies have suggested functional significance of galectin-1 in the reduced form during neural development and regeneration. For example, recombinant reduced galectin-1, when used as a coating substrate, promoted adhesion, aggregation and neurite fasciculation of neonatal rat DRG neurons (Outenreath & Jones, 1992) and olfactory neurons (Mahanthappa *et al.*, 1994; Puche *et al.*, 1996). On the other hand, little

attention has been paid to the oxidized form, which was considered to lack biological activities. Our recent findings shed light on oxidized galectin-1 as a novel neurotrophic molecule for mature sensory and motor neurons: recombinant human oxidized galectin-1 stimulated axonal regeneration and Schwann cell migration from the transected nerve stumps *in vivo* (Horie *et al.*, 1999; Fukaya *et al.*, 2003) and *in vitro* (Inagaki *et al.*, 2000). Because oxidized galectin-1 enhanced neurite outgrowth from transected nerve terminals of DRG explants but not from dissociated DRG neurons (Horie *et al.*, 1999), it is likely to stimulate non-neuronal cells to initiate axonal regeneration rather than act directly on neurons. Further studies are needed to clarify the action mechanisms of oxidized galectin-1 for the promotion of neural regeneration.

In summary, the results in the present study suggest that galectin-1 is externalized from neurons and Schwann cells of mature DRG *in vitro*. Some of the galectin-1 molecules in the extracellular space may be converted to the oxidized form, which loses lectin activity but displays neurotrophic function as a cytokine-like molecule. Due to its potent activity on neural regeneration, oxidized galectin-1 may play a pivotal role in restoration of peripheral nerve lesions caused by trauma and surgical operation (Horie & Kadoya, 2000; Fukaya *et al.*, 2003).

Acknowledgements

Abbreviations

CHO (cells), Chinese hamster ovary (cells); DRG, dorsal root ganglia; PBS, phosphate-buffered saline; RT-PCR, reverse transcription–polymerase chain reaction.

References

Avellana-Adalid, V., Rebel, G., Caron, M., Cornillot, J.-D., Bladier, D. & Joubert-Caron, R. (1994) Changes in S-type lectin localization in neuroblastoma cells (NIE115) upon differentiation. *Glycoconjugate J.*, 11, 286–291.

Barondes, S.H., Castronovo, V., Cooper, D.N.W., Cummings, R.D., Drickamer, K., Feizi, T., Gitt, M.A., Hirabayashi, J., Hughes, C., Kasai, K., Leffler, H., Liu, F., Lotan, R., Mercurio, A.M., Monsigny, M., Pillai, S., Poirer, F., Raz, A., Rigby, P.W.J. & Wang, J.L. (1994) Galectins: a family of animal β-galactoside-binding lectins. *Cell*, 76, 597–598.

Camby, I., Belot, N., Rorive, S., Lefranc, F., Maurage, C.A., Lahm, H., Kaltner, H., Hadari, Y., Ruchoux, M.M., Brotchi, J., Zick, Y., Salmon, I., Gabius, H.J. & Kiss, R. (2001) Galectins are differentially expressed in supratentorial pilocytic astrocytomas, astrocytomas, anaplastic astrocytomas and glioblastomas, and significantly modulate tumor astrocyte migration. *Brain Pathol.*, 11, 12–26.

Chi, H., Horie, H., Hikawa, N. & Takenaka, T. (1993) Isolation and age-related characterization of mouse Schwann cells from dorsal root ganglion explants in type I collagen gels. *J. Neurosci. Res.*, 35, 183–187.

Cho, M. & Cummings, R.D. (1995) Galectin-1, a β-galactoside-binding lectin in Chinese hamster ovary cells. *J. Biol. Chem.*, 270, 5207–5212.

Clerch, L.B., Whitney, P., Hass, M., Brew, K., Miller, T., Werner, R. & Massaro, D. (1988) Sequence of a full-length cDNA for rat lung β-galactoside-binding protein: primary and secondary structure of the lectin. *Biochemistry*, 27, 692–699.

Cleves, A.E., Cooper, D.N.W., Barondes, S.H. & Kelly, R.B. (1996) A new pathway for protein export in *Saccharomyces cerevisiae*. *J. Cell Biol.*, 133, 1017–1026.

Cooper, D.N.W. & Barondes, S.H. (1990) Evidence for export of a muscle lectin from cytosol to extracellular matrix and for a novel secretory mechanism. *J. Cell Biol.*, 110, 1681–1691.

Cooper, D.N.W. & Barondes, S.H. (1999) God must love galectins; he made so many of them. *Glycobiology*, 9, 979–984.

Danielsen, E.M. & van Deurs, B. (1997) Galectin-4 and small intestinal brush border enzymes from clusters. *Mol. Biol. Cell*, 8, 2241–2251.

Fukaya, K., Hasegawa, M., Kadoya, T., Horie, H., Fujisawa, H., Hayashi, Y., Tachibana, O., Kida, S. & Yamashita, J. (2003) Oxidized galectin-1 stimulates the migration of Schwann cells from both proximal and distal stumps of transected nerves and promotes axonal regeneration after peripheral nerve injury. *J. Neuropathol. Exp. Neurol.*, 62, 162–172.

Guizar-Sahagun, G., Garcia-Lopez, P., Espitia, A.L., Grijalva, I., Franco-Bourland, R.E. & Madrazo, I. (1998) Transitory expression of NAPDH diaphorase (NOS) in axonal swellings after spinal cord injury. *Neuroreport*, 9, 2899–2902.

Horie, H., Ikuta, S. & Takenaka, T. (1990) Membrane elasticity of mouse dorsal root ganglion neurons decreases with aging. *FEBS Lett.*, 269, 23–25.

Horie, H., Inagaki, Y., Sohma, Y., Nozawa, R., Okawa, K., Hasegawa, M., Muramatsu, N., Kawano, H., Horie, M., Koyama, H., Sakai, I., Takeshita, K., Kowada, Y., Takano, M. & Kadoya, T. (1999) Galectin-1 regulates initial axonal growth in peripheral nerves after axotomy. *J. Neurosci.*, 19, 9964–9974.

Horie, H. & Kadoya, T. (2000) Identification of oxidized galectin-1 as an initial repair regulatory factor after axotomy in peripheral nerves. *Neurosci. Res.*, 38, 131–137.

Hughes, R.C. (1999) Secretion of the galectin family of mammalian carbohydrate-binding proteins. *Biochem. Biophys. Acta*, 1473, 172–185.

Hynes, M.A., Gitt, M., Barondes, S.H., Jessell, T.M. & Buck, L.B. (1990) Selective expression of an endogenous lactose-binding lectin gene in subsets of central and peripheral neurons. *J. Neurosci.*, 10, 1004–1013.

Ichikawa, T., Ajiki, K., Matsuura, J. & Misawa, H. (1997) Localization of two cholinergic markers, choline acetyltransferase and vesicular acetylcholine transporter in the central nervous system of the rat: in situ hybridization histochemistry and immunohistochemistry. *J. Chem. Neuroanat.*, 13, 23–39.

Inagaki, Y., Sohma, Y., Horie, H., Nozawa, R. & Kadoya, T. (2000) Oxidized galectin-1 promotes axonal regeneration in peripheral nerves but does not possess lectin properties. *Eur. J. Biochem.*, 267, 2955–2964.

Kasai, K. & Hirabayashi, J. (1996) Galectins: a family of animal lectins that decipher glycocodes. *J. Biochem.*, 119, 1–8.

Kashiba, H., Hyon, B. & Senba, E. (1998) Glial cell line-derived neurotrophic factor and nerve growth factor receptor mRNAs are expressed in distinct subgroups of dorsal root ganglion neurons and are differentially regulated by peripheral axotomy in the rat. *Neurosci. Lett.*, 252, 107–110.

Kasper, M., Tonge, D. & Gordon-Weeks, P.R. (1999) Regeneration of adult dorsal root ganglion axons in explant culture. In Haynes, L.W. (ed.), *The Neuron in Tissue Culture*. John Wiley & Sons Ltd, Chichester, pp. 74–86.

Kawano, H., Fukuda, T., Kubo, K., Horie, M., Uyemura, K., Takeuchi, K., Osumi, N., Eto, K. & Kawamura, K. (1999) Pax-6 is required for thalamocortical pathway formation in fetal rats. *J. Comp. Neurol.*, 408, 147–160.

Kitchener, P.D., Wilson, P. & Snow, P.J. (1994) Sciatic axotomy compromises axonal transport of transganglionic tracer BSI-B4 from the soma to the central terminals of C fibre afferents. *Neurosci. Lett.*, 166, 121–125.

Lahm, H., Andre, S., Hoeflich, A., Fischer, J.R., Sordat, B., Kaltner, H., Wolf, E. & Gabius, H.J. (2001) Comprehensive galectin fingerprinting in a panel of 61 human tumor cell lines by RT-PCR and its implications for diagnostic and therapeutic procedures. *J. Cancer Res. Clin. Oncol.*, 127, 375–386.

Lindsay, R.M. (1988) Nerve growth factors (NGF, BDNF) enhance axonal regeneration but are not required for survival of adult sensory neurons. *J. Neurosci.*, 8, 2394–2405.

Llewellyn-Smith, I.J., Costa, M. & Furness, J.B. (1985) Light and electron microscopic immunocytochemistry of the same nerves from whole mount preparations. *J. Histochem. Cytochem.*, 33, 857–866.

Lutomski, D., Fouillit, M., Bourin, P., Mellottee, D., Denize, N., Pontet, M., Bladier, D., Caron, M. & Joubert-Caron, R. (1997) Externalization and binding of galectin-1 on cell surface of K562 cells upon erythroid differentiation. *Glycobiology*, 7, 1193–1199.

Mahanthappa, N.K., Cooper, D.N.W., Barondes, S.H. & Schwarting, G.A. (1994) Rat olfactory neurons can utilize the endogenous lectin, L-14, in a novel adhesion mechanism. *Development*, 120, 1373–1384.

Mehul, B. & Hughes, R.C. (1997) Plasma membrane targetting, vesicular budding and release of galectin 3 from the cytoplasm of mammalian cells during secretion. *J. Cell Sci.*, 110, 1169–1178.

Oorschot, D.E. & Jones, D.G. (1986) Tissue culture analysis of neurite outgrowth in the presence and absence of serum: possible relevance for central nervous system regeneration. *J. Neurosci. Res.*, 15, 341–352.

Outenreath, R.L. & Jones, A.L. (1992) Influence of an endogenous lectin substrate on cultured dorsal root ganglion cells. *J. Neurocytol.*, 21, 788–795.

Perillo, N.L., Marcus, M.E. & Baum, L.G. (1998) Galectins: versatile modulators of cell adhesion, cell proliferation, and cell death. *J. Mol. Med.*, 76, 402–412.

Perillo, N.L., Pace, K.E., Seihamer, J.L. & Baum, L.G. (1995) Apoptosis of T-cells mediated by galectin-1. *Nature*, 378, 736–739.

Pesheva, P., Kuklinski, S., Schmitz, B. & Probstmeier, R. (1998) Galectin-3 promotes neural cell adhesion and neurite growth. *J. Neurosci. Res.*, 54, 639–654.

Puche, A.C., Poirier, F., Hair, M., Bartlett, P.F. & Key, B. (1996) Role of galectin-1 in the developing mouse olfactory system. *Dev. Biol.*, 179, 274–287.

Rabinovich, G.A., Alonso, C.R., Sotomayor, C.E., Durand, S., Bocco, J.L. & Riera, C.M. (2000a) Molecular mechanisms implicated in galectin-1-induced apoptosis: activation of the AP-1 transcription factor and downregulation of Bcl-2. *Cell Death Differ.*, 7, 747–753.

Rabinovich, G.A., Baum, L.G., Tinari, N., Paganelli, R., Natoli, C., Liu, F.T. & Iacobelli, S. (2002) Galectins and their ligands: amplifiers, silencers or tuners of the inflammatory response? *Trends Immunol.*, 23, 313–320.

Rabinovich, G.A., Sotomayor, C.E., Riera, C.M., Bianco, I. & Correa, S.G. (2000b) Evidence of a role for galectin-1 in acute inflammation. *Eur. J. Immunol.*, 30, 1331–1339.

Regan, L.J., Dodd, J., Barondes, S.H. & Jessell, T.M. (1986) Selective expression of endogenous lactose-binding lectins and lactoseries glycoconjugates in subsets of rat sensory neurons. *Proc. Natl. Acad. Sci. USA*, 83, 2248–2252.

Salt, T.E. & Hill, R.G. (1983) Neurotransmitter candidates of somatosensory primary afferent fibers. *Neuroscience*, 10, 1083–1103.

Sango, K., Horie, H., Saito, H., Ajiki, K., Tokashiki, A., Takeshita, K., Ishigatsubo, Y., Kawano, H. & Ishikawa, Y. (2002b) Diabetes is not a potent inducer of neuronal cell death in mouse sensory ganglia, but it enhances neurite regeneration in vitro. *Life Sci.*, 71, 2351–2368.

Sango, K., Horie, H., Sotelo, J.R. & Takenaka, T. (1991) A high glucose environment improves survival of diabetic neurons in culture. *Neurosci. Lett.*, 129, 277–280.

Sango, K., Oohira, A., Ajiki, K., Tokashiki, A., Horie, M. & Kawano, H. (2003) Phosphacan and neurocan are repulsive substrata for adhesion and neurite extension of adult rat dorsal root ganglion neurons in vitro. *Exp. Neurol.*, 182, 1–11.

Sango, K., Yamanaka, S., Ajiki, K., Tokashiki, A. & Watabe, K. (2002a) Lysosomal storage results in impaired survival but normal neurite outgrowth in dorsal root ganglion neurons from a mouse model of Sandhoff disease. *Neuropathol. Appl. Neurobiol.*, 28, 23–34.

Senba, E., Imbe, H., Kami, K. & Morikawa, Y. (2001) Expression and functions of Galectin-1 in injured afferent system and muscles. *Neurosci. Res. Suppl.*, 25, S30–4.

Sotelo, J.R., Horie, H., Ito, S., Benech, C., Sango, K. & Takenaka, T. (1991) An in vitro model to study diabetic neuropathy. *Neurosci. Lett.*, 129, 91–94.

Toba, Y., Horie, M., Sango, K., Tokashiki, A., Matsui, F., Oohira, A. & Kawano, H. (2002) Expression and immunohistochemical localization of heparan sulfate proteoglycan N-syndecan in the migratory pathway from the rat olfactory placode. *Eur. J. Neurosci.*, 15, 1461–1473.

Tracey, B.M., Feizi, T., Abbott, W.M., Carruthers, R.A., Green, B.N. & Lawson, A.M. (1992) Subunit molecular mass assignment of 14,654 Da to the soluble beta-galactoside-binding lectin from bovine heart muscle and demonstration of intramolecular disulfide bonding associated with oxidative inactivation. *J. Biol. Chem.*, 267, 10342–10347.

de Waard, A., Hickman, S. & Kornfeld, S. (1976) Isolation and properties of beta-galactoside binding lectins of calf heart and lung. *J. Biol. Chem.*, 251, 7581–7587.

Watabe, K., Fukuda, T., Tanaka, J., Honda, H., Toyohara, K. & Sakai, O. (1995) Spontaneously immortalized adult mouse Schwann cells secrete autocrine and paracrine growth-promoting activities. *J. Neurosci. Res.*, 41, 279–290.

Watabe, K., Fukuda, T., Tanaka, J., Toyohara, K. & Sakai, O. (1994) Mitogenic effects of platelet-derived growth factor, fibroblast growth factor, transforming growth factor-β, and heparin-binding serum factor for adult mouse Schwann cells. *J. Neurosci. Res.*, 39, 525–534.

Watabe, K., Sakamoto, T., Kawazoe, Y., Michikawa, M., Miyamoto, K., Yamamura, T., Saya, H. & Araki, N. (2003) Tissue culture methods to study neurological disorders: Establishment of immortalized Schwann cells from murine disease models. *Neuropathology*, 23, 68–78.

Wilson, T.J.G., Firth, M.N., Powell, J.T. & Harrison, F.L. (1989) The sequence of the 14 kDa β-galactoside-binding lectin and evidence for its synthesis on free cytoplasmic ribosomes. *Biochem. J.*, 261, 847–852.

Zajc Kreft, K., Kreft, S., Komel, R. & Grubic, Z. (2000) Nonradioactive northern blotting for the determination of acetylcholinesterase mRNA. Comparison to the radioactive technique. *Pflugers Arch.*, 439 (Suppl.), R66–R67.

RESEARCH ARTICLE

Postischemic administration of Sendai virus vector carrying neurotrophic factor genes prevents delayed neuronal death in gerbils

M Shirakura[1,2], M Inoue[1], S Fujikawa[1], K Washizawa[1], S Komaba[1], M Maeda[3], K Watabe[4], Y Yoshikawa[2] and M Hasegawa[1]

[1]DNAVEC Research Inc., Tsukuba, Japan; [2]Department of Biomedical Science, Graduate School of Agricultural and Life Sciences, University of Tokyo, Tokyo, Japan; [3]First Department of Anatomy, Osaka City University Medical School, Osaka, Japan; and [4]Department of Molecular Neuropathology, Tokyo Metropolitan Institute for Neuroscience, Tokyo, Japan

Sendai virus (SeV) vector-mediated gene delivery of glial cell line-derived neurotrophic factor (GDNF) and nerve growth factor (NGF) prevented the delayed neuronal death induced by transient global ischemia in gerbils, even when the vector was administered several hours after ischemia. Intraventricular administration of SeV vector directed high-level expression of the vector-encoded neurotrophic factor genes, which are potent candidates for the treatment of neurodegenerative diseases. After occlusion of the bilateral carotid arteries of gerbils, SeV vector carrying GDNF (SeV/GDNF), NGF (SeV/NGF), brain-derived neurotrophic factor (SeV/BDNF), insulin-like growth factor-1 (SeV/IGF-1) or vascular endothelial growth factor (SeV/VEGF) was injected into the lateral ventricle. Administration of SeV/GDNF, SeV/NGF or SeV/BDNF 30 min after the ischemic insult effectively prevented the delayed neuronal death of the hippocampal CA1 pyramidal neurons. Furthermore, the administration of SeV/GDNF or SeV/NGF as late as 4 or 6 h after the ischemic insult also prevented the death of these neurons. These results indicate that SeV vector-mediated gene transfer of neurotrophic factors has high therapeutic potency for preventing the delayed neuronal death induced by transient global ischemia, and provides an approach for gene therapy of stroke.

Gene Therapy (2004) 11, 784-790. doi:10.1038/sj.gt.3302224
Published online 12 February 2004

Neurons are postmitotic and highly differentiated, and are extremely vulnerable to ischemic injury. Pyramidal cells of the hippocampal CA1 region are well known to be especially vulnerable to cerebral ischemia.[1,2] Neuronal cell death in the CA1 region itself is not death-dealing but results in severe deficits of memory function.[3–5] Since the regeneration of neuronal cells remains critically difficult at present, protection against the neuronal loss induced by ischemic injury is vital in cerebrovascular-type dementia.

Glial cell line-derived neurotrophic factor (GDNF) is a potent neurotrophic factor that promotes the cell survival and differentiation of dopaminergic neurons[6,7] and motoneurons.[8,9] Nerve growth factor (NGF) also has a potent ability to protect neurons from various injuries and promote the survival of cholinergic neurons.[10–12] These neurotrophic factors may be valuable as candidates for use in therapy of neurodegenerative diseases. It has been reported that the neuronal cell death induced by ischemic injury was prevented by the administration of GDNF[13–15] and NGF[16–18] proteins. However, the usefulness of such protein factors in patients is limited because of their poor bioavailability and short half-lives.

Moreover, these agents might be ineffective without direct injection and continuous infusion into the ventricle, striatum or cerebral cortex. Therefore, virus vector-mediated gene transfer is expected to be an effective approach for the delivery of therapeutic proteins into the central nervous system (CNS). Even in the case of unsustained, but transient, expression by the vectors, it would enable significant cutting down of the number of required administrations. Previous studies demonstrated that gene transfer of neurotrophic factors such as GDNF[19] and NGF[20,21] rescued neuronal cells from ischemic injury in animal models. However, there have not been any reports in which neurotrophic factors expressed using conventional vectors such as adenovirus, retrovirus or adeno-associated virus were shown to promote the survival of neurons when the vectors were administered after ischemia.

We have developed a new type of gene transfer vector using Sendai virus (SeV), which is classified as a type I parainfluenza virus belonging to the family Paramyxoviridae with a negative-strand RNA genome.[22,23] SeV has a strictly cytoplasmic life cycle in mammalian cells, that is, its genomic RNA is restricted to the cytoplasm and has no interaction with the host chromosomes.[22] Therefore, SeV vector causes no genotoxicity such as the permanent integration in the target cells sometimes observed with other conventional viral

vectors. SeV has the ability to infect most mammalian cells such as neuronal and muscular cells and directs high-level gene expression in these cells.[23–26] Indeed, we observed potent infectivity of SeV vector in ependymal cells after intraventricular administration in the CNS.[27] When the SeV vector carrying enhanced green fluorescent protein gene (SeV/GFP) was administered into the left lateral ventricle of gerbils, intense GFP expression was observed around the ependymal layer of the lateral ventricles (Figure 1c) and around the hippocampus (Figure 1b). Immunohistochemical analysis using anti-SeV antibody clearly showed that the cells supporting SeV replication were ependymal cells in the lateral ventricles (Figure 1d), third ventricle (Figure 1e) and around the hippocampus (Figure 1f). We previously showed that SeV vector-mediated gene transfer of GDNF 4 days before transient ischemia prevented the delayed neuronal death induced by transient global ischemia in gerbils.[27] However, SeV vector was administered prior to the ischemic insult in that case, too, whereas gene therapy must be applied after the occurrence of a stroke for clinical application. In the present study, we examined the effects of postischemic administration of SeV vectors carrying GDNF, NGF and other neurotrophic factor genes on the delayed neuronal death induced by transient global ischemia. Our results suggest that SeV vector-mediated gene transfer has a therapeutic high potential for cerebral ischemia.

In order to confirm the efficient gene transfer and expression of SeV in the CNS, the proteins derived from the genes harbored in the SeV vector were quantified. SeV vectors such as SeV/GDNF, SeV/NGF and SeV/GFP were administered into the left lateral ventricle of gerbils at 5×10^6 PFU/head, and the amount of GDNF and NGF proteins in the hippocampus was quantified by ELISA assays. High-level expression of GDNF (114 ± 6 pg/mg tissue) and NGF (1130 ± 60 pg/mg tissue) proteins was detected in the hippocampus of gerbils as early as 1 day after injection of SeV/GDNF and SeV/NGF, respectively (Figure 2a, b). In contrast, only a very small amount of GDNF or NGF protein was detected when the gerbils were treated with SeV/GFP. The expression of GDNF (2340 ± 200 pg/mg tissue) and NGF (3360 ± 290 pg/mg tissue) proteins reached peak levels 4 days after injection of SeV/GDNF and SeV/NGF, respectively, and then returned to the original level 14 days after the injection. In another experiment, an increment of GDNF expression in the cerebrospinal fluid was detected 8 h after injection of SeV/GDNF (data not shown). These results indicate that rapid and high-level expression of neurotrophic factors can be achieved by the administration of SeV vectors in the CNS. Also, the expression level achieved using SeV vectors was remarkably high compared with that achieved using adenovirus. For example, the GDNF concentration was reported to be 2.2 ± 0.5 pg/mg tissue 1 day after the
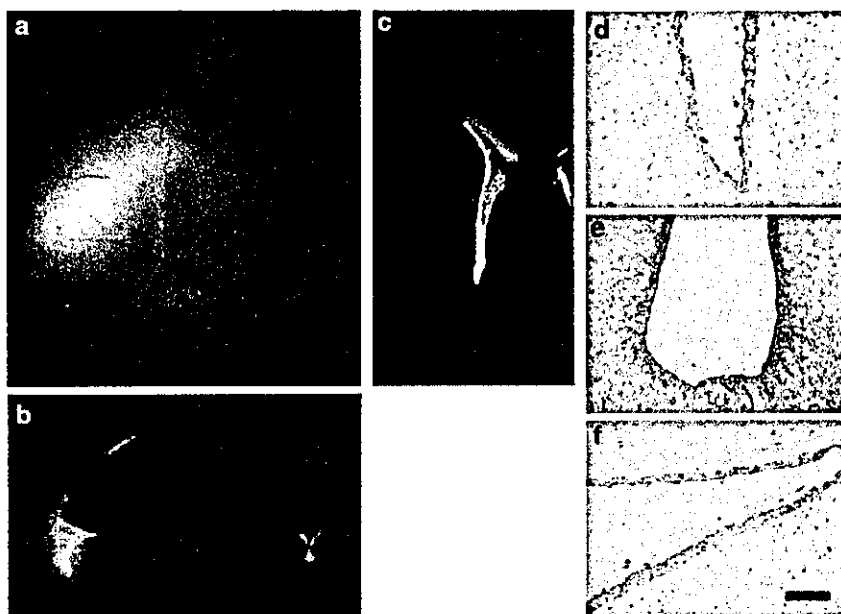
Figure 1 Identification of cell types supporting SeV replication. SeV vector carrying GFP gene (SeV/GFP; 5×10^6 PFU/head) was injected into the left lateral ventricle of gerbils as described previously,[27] and the GFP expression 4 days after the injection was observed under a stereoscopic fluorescence microscope (Leica, Germany) from the surface of the top of brain (a) and with coronal sections around the hippocampus (b) and lateral ventricle (c). For the coronal sections, the brain was sliced into 300-μm-thick slices with a microslicer (DTK-1000; Dosaka, Japan). Representative photographs of immunohistochemical staining for SeV are shown (d–f). The paraffin sections were pretreated with 0.3% H_2O_2 in PBS, followed by washing thrice. After blocking with 10% normal goat serum (NGS) in PBS for 1 h, the sections were incubated overnight at 4°C with a rabbit polyclonal antibody to SeV (anti-SeV)[28] in 3% NGS and 0.3% Triton X-100 in PBS. The sections were then washed and incubated for 1 h with biotinylated anti-rabbit IgG (Vector Laboratories, Burlingame, CA, USA), followed by incubation for 1 h with the reagents for avidin–biotin complex formation (Vector Laboratories). Immunopositive cells were visualized by reaction with 3,3'-diaminobenzidine tetrahydrochloride (DAB) (WAKO Pure Chmicals, Tokyo, Japan) and counterstained with hematoxylin. Scale bars = 100 μm. The ependymal cells along the (d) lateral ventricle, (e) third ventricle and (f) hippocampus were SeV positive.
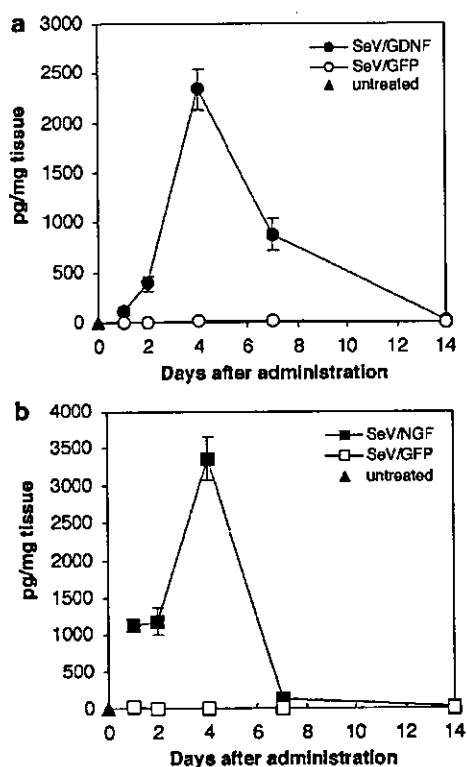
786

injection into the cortex of adenovirus $(1 \times 10^8 \text{ PFU}/$ head) carrying the GDNF gene.[29]

We next examined the effects of the postischemic administration of SeV vectors on the delayed neuronal death of the hippocampal CA1 pyramidal cells induced by transient ischemia. It has been reported that the direct administration of the bcl-2 gene mediated by adeno-associated virus (AAV) into pyramidal neurons within 1 h after ischemic insult prevents the delayed neuronal death in gerbils.[30] However, direct injection of virus vectors into the cerebral parenchyma cells, especially in

Figure 2 Kinetics of the expression of GDNF and NGF proteins in the hippocampus. Gerbils were injected with SeV vectors carrying GDNF (SeV/GDNF), NGF (SeV/NGF) or GFP (SeV/GFP) genes $(5 \times 10^6 \text{ PFU}/$ head, $n = 20$ animals per group) into the left lateral ventricle as described.[27] At 1, 2, 4, 7 or 14 days after the injection, the concentrations of GDNF and NGF in the hippocampus were measured using ELISA kits (Promega, WI, USA) as previously described.[27] The hippocampus was harvested from four gerbils at each time point. SeV/GDNF and SeV/GFP were constructed as previously described.[27] SeV/NGF was constructed as described.[27,28] Briefly, mouse NGF (accession number: M14805) cDNA was amplified with a pair of NotI-tagged (underlined) primers containing SeV-specific transcriptional regulatory signal sequences, 5'-ACTTG CGGCCGCCAAAGTTCAGTAATGTCCATGTTGTTCTACACTCTG-3' and 5'-ATCCGCGGCCGCGATGAACTTTCACCCTAAGTTTTTCTTA CTACGGTCAGCCTCTTCTTGTAGCCTTCCTGC-3'. The amplified fragment was introduced into the NotI site of the parental pSeV18⁺b(+), +), which was constructed to produce the exact SeV full-length antigenomic RNA, to generate pSeV/NGF. pSeV/NGF was transfected into LLC-MK₂ cells after infection of the cells with vaccinia virus vTF7-3, which expresses T7 polymerase. The T7-driven full-length recombinant SeV/NGF RNA genomes were encapsulated by NP, P and L proteins, which were derived from the respective cotransfected plasmids. After incubation for 40 h, cell lysates of transfected cells were injected into embryonated chicken eggs to amplify the recovered viruses. The virus titers were determined using a hemagglutination units (HAU) assay. Values are expressed as the mean ± s.d.

the hippocampus, is more invasive than intraventricular administration. Therefore, we selected a single intraventricular administration and utilized SeV-transduced ependymal cells to produce proteins from the genes carried by the vectors.[27] Accordingly, SeV/GDNF and SeV/NGF $(5 \times 10^6 \text{ PFU}/\text{head})$ were injected into the lateral ventricles of ischemic gerbils after 30 min of occlusion of the bilateral carotid arteries, and histopathological analysis was conducted 6 days after the injection. The effects of the above vectors were compared with those of SeV vectors carrying brain-derived neurotrophic factor (SeV/BDNF), insulin-like growth factor-1 (SeV/IGF-1) and vascular endothelial growth factor (SeV/VEGF). All the genes carried by the vectors have been reported to prevent neuronal degeneration after transient ischemia,[31–33] and for each SeV vector, vector-derived expression in infected cells was confirmed *in vitro* (data not shown). In sham-operated gerbils, surviving wheel-like nuclei were observed in the pyramidal cells in CA1 (Figure 3a). However, in gerbils treated with SeV/GFP, almost all of the pyramidal cells in the hippocampal CA1 region showed pyknotic degenerative nuclei in the pyramidal cells (Figure 3g). In contrast, treatment of gerbils with SeV/GDNF or SeV/NGF ameliorated the delayed neuronal death in the hippocampal CA1 pyramidal cells (Figure 3b, c). Treatment with SeV/BDNF also showed ameliorative effects (Figure 3d), but treatment with SeV/VEGF did not (Figure 3f). Treatment with SeV/IGF-1 showed ameliorative effects (Figure 3e) in only two gerbils among eight tested. For quantitative analysis, the number of surviving neurons/1-mm length in the hippocampal CA1 region was counted (Figure 4). Treatment with SeV/GDNF $(180.8 \pm 11.7 \text{ cells}/\text{mm})$ or SeV/NGF $(142.4 \pm 24.3 \text{ cells}/\text{mm})$ significantly prevented neuronal death as compared to treatment with SeV/GFP $(10.7 \pm 1.9 \text{ cells}/\text{mm})$ $(P < 0.01)$. Treatment with SeV/BDNF $(139.3 \pm 29.7 \text{ cells}/\text{mm})$ also reduced the cell death of the neurons by about 70%. SeV/GDNF and SeV/NGF (and SeV/BDNF) proved to be better for the treatment of transient global ischemia than SeV vectors carrying genes for the other factors investigated here. As a way to confirm that the vector-derived growth factors actually increased and acted to prevent the neuronal death of the hippocampal CA1 pyramidal neurons, we measured the concentrations of both NGF and GDNF proteins in the hippocampus of 'ischemic' gerbils 4 days after the injection of SeV/GDNF or SeV/NGF into the lateral ventricle. When the SeV/GDNF was injected at 4 h after ischemia, the concentration of GDNF $(71.9 \pm 12.0 \text{ pg}/\text{mg}$ tissue) was increased compared to that of SeV/GFP-injected $(0.057 \pm 0.022 \text{ g}/\text{mg}$ tissue) or untreated $(0.038 \pm 0.042 \text{ pg}/\text{mg}$ tissue) gerbils. However, the concentration of NGF $(15.8 \pm 0.9 \text{ pg}/\text{mg}$ tissue) remained at the original level of SeV/GFP-injected $(15.4 \pm 4.6 \text{ pg}/\text{mg}$ tissue) or untreated $(18.2 \pm 6.2 \text{ pg}/\text{mg}$ tissue) gerbils. When the SeV/NGF was injected at 4 h after ischemia, the concentration of NGF $(1570 \pm 210 \text{ pg}/$ mg tissue) but not that of GDNF $(0.074 \pm 0.047 \text{ pg}/\text{mg}$ tissue) increased, and this NGF could show a neuroprotective effect. These results indicate that the vector-derived growth factors rather than the intrinsic ones increase and function to prevent the neuronal death.

To examine the effect of extending the time until the administration of SeV vectors after ischemic insult, which is important for practical use in clinical applications,

SeV/GDNF and SeV/NGF were injected 4 h after ischemia. Surviving neurons in the hippocampal CA1 region were observed in gerbils treated with either SeV/GDNF or SeV/NGF, although a few degenerated nuclei of neurons were observed in these cases (Figure 5b, c). The number of surviving neurons in the hippocampal CA1 region was also counted (Figure 6). Administration of SeV/GDNF (114.7±9.7 cells/mm) or SeV/NGF (127.6±13.8 cells/mm) prevented the neuronal death as compared to administration of SeV/GFP (14.3±5.6 cells/mm) (P<0.01), even if the vectors were administered 4 h after ischemia. Moreover, treatment with SeV/GDNF (74.2±9.6 cells/mm) or SeV/NGF (76.4±10.8 cells/mm) 6 h after ischemic insult was also effective for prevention of the delayed neuronal death as compared to treatment with SeV/GFP (11.7±2.3 cells/mm) (P<0.01) (Figure 5e, f and Figure 6). Equal neuroprotective effects were observed on the ipsilateral and contralateral sides of the hippocampal CA1 region (data not shown), indicating that the proteins expressed by SeV vectors were extensively dispersed. These results indicate that administration of SeV/GDNF or SeV/NGF even several hours after ischemia effectively prevents the delayed neuronal death induced by transient global ischemia. There have been no previous reports showing that the administration of virus vector-mediated genes at 4 h or even 6 h after an ischemic insult was effective for preventing the delayed neuronal death induced by transient ischemia in animal models. Our results indicate that the time window for the treatment of cerebral ischemia could be substantially extended. It was reported that more than 8 h was required for the expression of genes carried by adenovirus vectors in the rat brain.[34] Thus, the time needed for expression of genes carried by SeV vector

may be shorter than that needed for genes carried by adenovirus vector. The rapid gene expression achieved using SeV vectors may be due to the rapid replication, high level of mRNA transcription and effective translation of the mRNA of the vectors, that is, the typical features of RNA viruses. This may have led to the protective effect observed even with 6 h postischemic administration of SeV vectors against the delayed
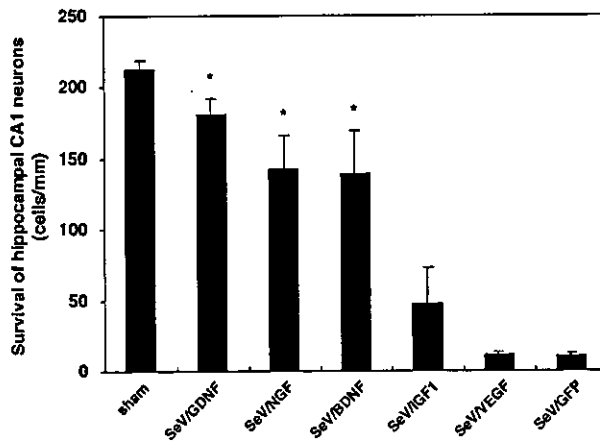

Figure 4 Quantitative analysis of the effect of SeV vector on ischemic injury when administered 30 min after ischemia. SeV/GDNF, SeV/NGF, SeV/BDNF, SeV/IGF-1, SeV/VEGF or SeV/GFP was injected intraventricularly 30 min after ischemic insult. The number of surviving neurons/ 1-mm length in the hippocampal CA1 region was calculated. Values are expressed as the mean±s.d. (n=8 animals per group). Asterisks indicate a significant difference as compared with the SeV/GFP-treated group. (P<0.01, Student's t test).
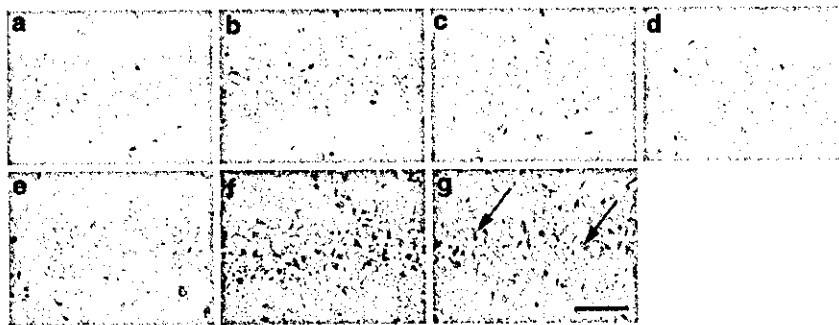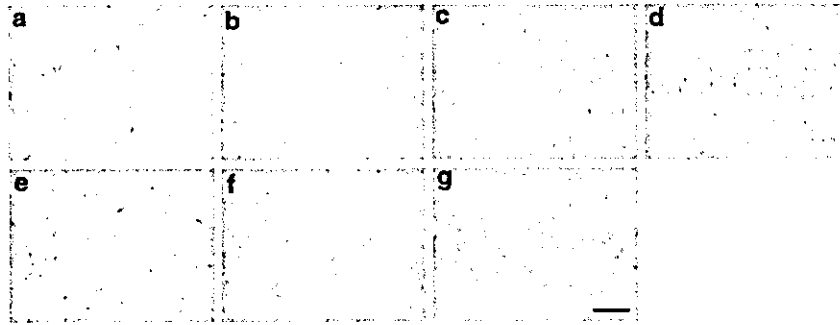

Figure 3 Representative photographs of pyramidal neurons in the hippocampal CA1 region after treatment (30 min after ischemia) with SeV vector following ischemic injury. (a) Sham-operated gerbils; (b) SeV/GDNF-, (c) SeV/NGF- (d) SeV/BDNF-, (e) SeV/IGF-1-, (f) SeV/VEGF- and (g) SeV/GFP-treated gerbils 30 min after ischemic insult. These sections were stained with hematoxylin and eosin. Arrows indicate the pyknotic nuclei of neurons. Scale bar = 50 μm. SeV vectors carrying the BDNF (SeV/BDNF), IGF-1 (SeV/IGF-1) and VEGF (SeV/VEGF) genes were constructed as described in Figure 1. In this experiment, human BDNF (accession number: XM_006027), human IGF-1 (accession number: X56773) and human VEGF (accession number: AY047581) cDNAs were amplified with a pair of NotI-tagged (underlined) primers containing SeV-specific transcriptional regulatory signal sequences, 5'-ACTTGCGGCCGCCAAAGTTCAGTGATGACCATCCTTTTCCTTAC-3' and 5'-ATCCGCGGCCGCGATGAACTTTCACCCTAAGTTTTTCTTAC TACGGCTATCTTCCCCTTTTAATGGTCAATGTAC-3' for BDNF, 5'-ACTTGCGGCCGCCAAAGTTCAGCAATGGGAAAAATCAGCAGTCTTC-3' and 5'-ATCCGCGGCCGCGATGAACTTTCACCCTAAGTTTTTCTTACTACGGCTACATCCTGTAGTTCTTGTTTCCTGC-3' for IGF-1 and 5'-ACTTGCGGCCGCCAAAGTTCACTAATGAACTTTCTGCTGTCTTGGGTGC-3' and 5'-ATCCGCGGCCGCGATGAACTTTCACCC TAAGTTTTTCTTACTACGGTCACCGCCTCGGCTTGTCACATCTGC-3' for VEGF. Adult male Mongolian gerbils (60-80 g) were used in this experiment. Occlusion of the bilateral common carotid arteries was performed as previously described.[19,27] Briefly, gerbils were anesthetized by an intraperitoneal injection of chloral hydrate (300 mg/kg)[19] and both common carotid arteries were clamped for 5 min with surgical clips to produce transient forebrain ischemia. The body temperature was measured using a thermocouple probe inserted into the anus and maintained at 37.5°C using a heating pad. Sham-operated animals were treated in the same manner except for occlusion of the bilateral common carotid arteries. At 30 min after the ischemic insults, SeV/GDNF, SeV/NGF, SeV/BDNF, SeV/IGF-1, SeV/VEGF or SeV/GFP (5 × 10^6 PFU/head, n = 8 animals per group) was injected intraventricularly into gerbils. At 6 days after injection, the gerbils were anesthetized with ether and transcardially perfused with normal saline followed by 4% paraformaldehyde in 0.1 M phosphate buffer (PB). The brains were removed and fixed in the same fixative overnight and then processed into paraffin blocks. Coronal brain sections were cut at 5-μm thickness and stained with hematoxylin and eosin. Arrows indicate the pyknotic nuclei of neurons. Scale bar = 50 μm.

Figure 5 Representative photographs of pyramidal neurons in the hippocampal CA1 regions after treatment (4 and 6 h after ischemia) with SeV vector following ischemic injury. SeV/GDNF (b, e), SeV/NGF (c, f) or SeV/GFP (d, g) was administered intraventricularly 4 h (b, c, d) or 6 h (e, f, g) after ischemic insult. The sections were stained with hematoxylin and eosin. Scale bar = 50 μm. Occlusion of the bilateral common carotid arteries was performed as described in Figure 2.

neuronal death of the hippocampal CA1 pyramidal neurons induced by transient ischemia. Moreover, these attractive features of SeV vectors may make them useful for the treatment of acute diseases such as cerebral ischemia.

It has been reported that NGF administration prevented the delayed neuronal death when neurons were observed 7 days after ischemic insult, but not when they were observed 28 days after the insult.[18] The long-term effects of the vectors studied here therefore had to be examined to better clarify their potential benefits in clinical use. Therefore, we also examined the long-term effects of SeV/GDNF and SeV/NGF on delayed neuronal death. The effect of SeV vectors for preventing neuronal death could be observed even when analyzed 28 days after the insult, although it was not seen in the case of topical application of NGF protein.[18] However, the number of surviving neurons at 28 days after the ischemia was reduced to almost half of that at 6 days after ischemia in the cases of gerbils treated with SeV/GDNF and SeV/NGF (Figure 7). High-level expression of the vector-encoded protein was detected after the administration of the SeV vector, but this expression reached a peak 4 days after the administration and then decreased to the basal level by 14 days. It is probable that immune responses induced by the virus particles or genes derived from SeV may cause the rapid decline of the gene expression of SeV. However, this limitation may be circumvented by the development of a new generation of SeV vectors that elicit weaker immune responses, which should extend the duration of gene expression. We have developed a series of an attenuated type of SeV vectors that are F gene-deleted,[24] F gene-deleted with preferable mutations,[35] M gene-deleted,[36] or have combinations of deletions of these genes (Kitazato K, unpublished; Inoue M, unpublished). We plan the first clinical application of SeV vector carrying human fibroblast growth factor-2 for the treatment of peripheral arterial disease using F gene-deleted SeV vector. As the F gene-deleted SeV is nontransmissible and shows less cytopathic effect than the wild-type SeV, we should utilize this type of SeV (or further advanced types of SeV vector) for applications to brain ischemia. Improvement of the vector modifications will ultimately provide better protection against ischemic injury. Moreover, alternative administration routes, such as lumbar puncture of the vectors, should be developed for the purposes of human
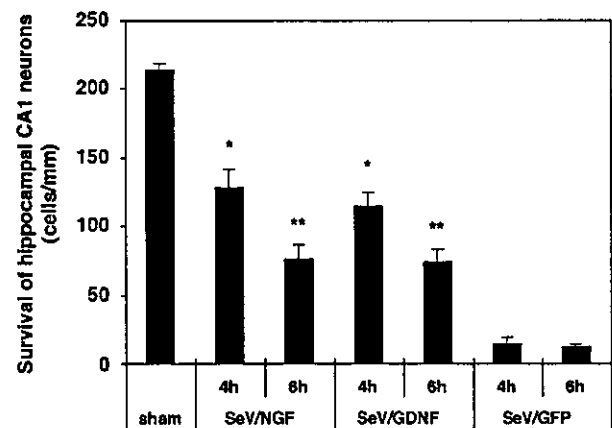
Figure 6 Quantitative analysis of the effect of SeV vector on ischemic injury when administered 4 and 6 h after ischemia. SeV/GDNF, SeV/NGF or SeV/GFP was injected intraventricularly 4 or 6 h after ischemic insult. The number of surviving neurons/1-mm length in the hippocampal CA1 region was calculated. Values are expressed as the mean±s.d. (n = 8 animals per group). Asterisks indicate a significant difference as compared with the SeV/GFP-treated group. (P<0.01, Student's t test).

gene therapy for cerebrovascular diseases. Hayashi and co-workers[37] reported that liposome-mediated hepatocyte growth factor (HGF) gene transfer into the subarachnoid space prevented delayed neuronal death in gerbils. Intrathecal injection into the cisterna magna involves no systematic anesthesia, no burr hole and no pain for patients. For use in clinical application, these methods should be tested in future studies. More importantly, we have already confirmed the efficient replication of SeV vectors in primates. In fact, high-level expression of GDNF (more than 100 ng/ml) was observed in cerebrospinal fluid after the injection of SeV vector carrying the GDNF gene (SeV/GDNF) into the lateral ventricle of primates (data not shown). Thus, we are going to evaluate the SeV/GDNF vector for its effects on the recovery from brain ischemia using primates. In such experiments, we hope to show a correlation between CA1 neuroprotection and functional recovery.

In conclusion, the present study demonstrated that postischemic administration of SeV vectors carrying genes for GDNF and NGF effectively prevented the delayed neuronal death of the hippocampal CA1
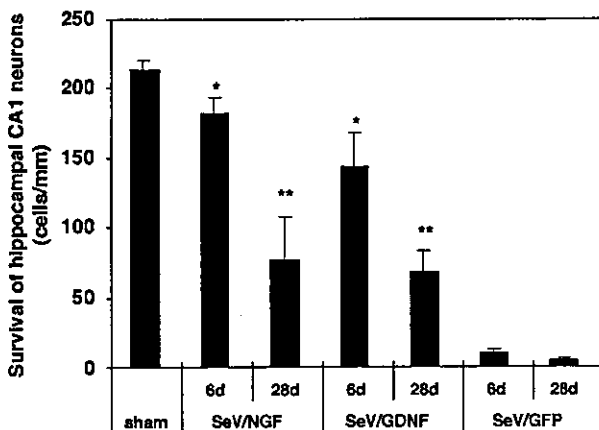
Figure 7 *Long-term effect of the SeV vectors on ischemic injury. SeV/ GDNF, SeV/NGF or SeV/GFP was injected intraventricularly 30 min after ischemic insult. At 6 days or 28 days after injection, gerbils were anesthetized, and the number of surviving neurons/1-mm length in the hippocampal CA1 region was calculated. Values are expressed as the mean±s.d. (n=8 animals per group). Asterisks indicate a significant difference as compared with the SeV/GFP-treated group. (P<0.01, Student's t test).*

pyramidal cells induced by occlusion of the bilateral carotid arteries. It is noteworthy that the neuroprotective effect was obtained even 4 and 6 h after ischemic insults. These results indicate that gene therapy using SeV vectors is of great potential usefulness for the treatment of cerebral ischemia.

Acknowledgements

References

1 Kirino T. Delayed neuronal death in the gerbil hippocampus following ischemia. Brain Res 1982; 239: 57–59.

2 Kirino T, Sano K. Selective vulnerability in the gerbil hippocampus following transient ischemia. Acta Neuropathol (Berl.) 1984; 62: 201–208.

3 Andersen MB, Sams-Dodd F. Impairment of working memory in the T-maze after transient global cerebral ischemia in the Mongolian gerbil. Behav Brain Res 1998; 91: 15–22.

4 Li AJ et al. Protective effect of acidic fibroblast growth factor against ischemia-induced learning and memory deficits in two tasks in gerbils. Physiol Behav 1999; 66: 577–583.

5 Catania MA et al. Erythropoietin prevents cognition impairment induced by transient brain ischemia in gerbils. Eur J Pharmacol 2002; 437: 147–150.

6 Beck KD et al. Mesencephalic dopaminergic neurons protected by GDNF from axotomy-induced degeneration in the adult brain. Nature 1995; 373: 339–341.

7 Choi-Lundberg DL et al. Dopaminergic neurons protected from degeneration by GDNF gene therapy. Science 1997; 275: 838–841.

8 Henderson CE et al. GDNF: a potent survival factor for motoneurons present in peripheral nerve and muscle. Science 1994; 266: 1062–1064.

9 Li L et al. Rescue of adult mouse motoneurons from injury-induced cell death by glial cell line-derived neurotrophic factor. Proc Natl Acad Sci USA 1995; 92: 9771–9775.

10 Fischer W et al. Amelioration of cholinergic neuron atrophy and spatial memory impairment in aged rats by nerve growth factor. Nature 1987; 329: 65–68.

11 Montero CN, Hefti F. Rescue of lesioned septal cholinergic neurons by nerve growth factor: specificity and requirement for chronic treatment. J Neurosci 1988; 8: 2986–2999.

12 Tuszynski MH, U HS, Amaral DG, Gage FH. Nerve growth factor infusion in the primate brain reduces lesion-induced cholinergic neuronal degeneration. J Neurosci 1990; 10: 3604–3614.

13 Abe K, Hayashi T, Itoyama Y. Amelioration of brain edema by topical application of glial cell line-derived neurotrophic factor in reperfused rat brain. Neurosci Lett 1997; 231: 37–40.

14 Kitagawa H et al. Reduction of ischemic brain injury by topical application of glial cell line-derived neurotrophic factor after permanent middle cerebral artery occlusion in rats. Stroke 1998; 29: 1417–1422.

15 Miyazaki H et al. Glial cell line-derived neurotrophic factor protects against delayed neuronal death after transient forebrain ischemia in rats. Neuroscience 1999; 89: 643–647.

16 Shigeno T et al. Amelioration of delayed neuronal death in the hippocampus by nerve growth factor. J Neurosci 1991; 11: 2914–2919.

17 Yamamoto S et al. Protective effect of NGF atelocollagen mini-pellet on the hippocampal delayed neuronal death in gerbils. Neurosci Lett 1992; 141: 161–165.

18 Ishimaru H et al. NGF delays rather than prevents the cholinergic terminal damage and delayed neuronal death in the hippocampus after ischemia. Brain Res 1998; 789: 194–200.

19 Yagi T et al. Rescue of ischemic brain injury by adenoviral gene transfer of glial cell line-derived neurotrophic factor after transient global ischemia in gerbils. Brain Res 2000; 885: 273–282.

20 Hermann DM et al. Adenovirus-mediated GDNF and CNTF pretreatment protects against striatal injury following transient middle cerebral artery occlusion in mice. Neurobiol Dis 2001; 8: 655–666.

21 Andsberg G et al. Neuropathological and behavioral consequences of adeno-associated viral vector-mediated continuous intrastriatal neurotrophin delivery in a focal ischemia model in rats. Neurobiol Dis 2002; 9: 187–204.

22 Lamb RA, Kolakofsky D. Paramyxoviridae: the virus and their replication. In: Fields BN, Knipe DM, Howley PM (eds) Fields Virology. Lippincott-Raven: Philadelphia, 1996, pp. 1177–1204.

23 Nagai Y, Kato A. Paramyxovirus reverses genetics is coming of age. Microbiol Immunol 1999; 43: 613–624.

24 Li HO et al. A cytoplasmic RNA vector derived from non-transmissible Sendai virus with efficient gene transfer and expression. J Virol 2000; 74: 6564–6569.

25 Yonemitsu Y et al. Efficient gene transfer to airway epithelium using recombinant Sendai virus. Nat Biotechnol 2000; 18: 970–973.

26 Shiotani A et al. Skeletal muscle regeneration after insulin-like growth factor I gene transfer by recombinant Sendai virus vector. Gene Therapy 2001; 8: 1043–1050.

27 Shirakura M et al. Sendai virus vector-mediated gene transfer of glial cell line-derived neurotrophic factor prevents delayed neuronal death after transient global ischemia in gerbils. Exp Anim 2003; 52: 119–127.

28 Kato A et al. Initiation of Sendai virus multiplication from transfected cDNA or RNA with negative or positive sense. Genes Cells 1996; 1: 569–579.

29 Kitagawa H et al. Adenovirus-mediated gene transfer of glial cell line-derived neurotrophic factor prevents ischemic brain injury after transient middle cerebral artery occlusion in rats. J Cereb Blood Flow Metab 1999; 19: 1336–1344.

790

30 Shimazaki K *et al.* Adeno-associated virus vector-mediated bcl-2 gene transfer into post-ischemic gerbil brain *in vivo*: prospects for gene therapy of ischemia-induced neuronal death. *Gene Therapy* 2000; **7**: 1244–1249.

31 Beck T *et al.* Brain-derived neurotrophic factor protects against ischemic cell damage in rat hippocampus. *J Cereb Blood Flow Metab* 1994; **14**: 689–692.

32 Wang JM *et al.* Reduction of ischemic brain injury by topical application of insulin-like growth factor-I after transient middle cerebral artery occlusion in rats. *Brain Res* 2000; **859**: 381–385.

33 Croll SD, Wiegand SJ. Vascular growth factors in cerebral ischemia. *Mol Neurobiol* 2001; **23**: 121–135.

34 Abe K *et al. In vivo* adenovirus-mediated gene transfer and the expression in ischemic and reperfused rat brain. *Brain Res* 1997; **763**: 191–201.

35 Inoue M *et al.* Non-transmissible virus-like particle formation by F-deficient Sendai virus is temperature-sensitive and reduced by mutations in M and HN proteins. *J Virol* 2003; **77**: 3238–3246.

36 Inoue M *et al.* A new Sendai virus vector deficient in the matrix gene does not form virus particles and shows extensive cell-to-cell spreading. *J Virol* 2003; **77**: 6419–6429.

37 Hayashi K *et al.* Gene therapy for preventing neuronal death using hepatocyte growth factor: *in vivo* gene transfer of HGF to subarachnoid space prevents delayed neuronal death in gerbil hippocampal CA1 neurons. *Gene Therapy* 2001; **8**: 1167–1173.

ELSEVIER

GALC transduction leads to morphological improvement of the twitcher oligodendrocytes in vivo

Xing-Li Meng[a], Jin-Song Shen[a], Kazuhiko Watabe[a,c], Toya Ohashi[a,b,*], Yoshikatsu Eto[a,b]

[a] Department of Gene Therapy, Institute of DNA Medicine, The Jikei University School of Medicine, Tokyo, Japan
[b] Department of Pediatrics, The Jikei University School of Medicine, Tokyo, Japan
[c] Department of Neuropathology, Tokyo Metropolitan Institute for Neuroscience, Tokyo, Japan

Abstract

Globoid cell leukodystrophy (GLD, Krabbe disease) is a severe demyelinating disease caused by a genetic defect of β-galacto-cerebrosidase (GALC). To date treatment to GLD is limited to hematopoietic stem cell transplantation. Experimental approaches by means of gene therapy in twitcher mouse, an authentic murine model of human GLD, showed significant but only marginal improvements of the disease. To clarify whether the introduction of GALC could provide beneficial effects on the oligodendrocytes in GLD, we transduced twitcher oligodendrocytes by stereotactically injecting recombinant retrovirus encoding GALC-myc-tag fusion gene into the forebrain subventricular zone of neonatal twitcher mouse. In vivo effects of exogenous GALC on twitcher oligodendrocytes were studied histologically by combined immunostaining for the myc-epitope and the oligodendroglial specific marker, π form of glutathione-S-transferase, at around 40 days of age. We show here that GALC transduction led to dramatic morphological improvement of the twitcher oligodendrocytes comparing with those in untreated twitcher controls. This study provided direct in vivo evidence that GALC transduction could prevent or correct aberrant morphology of oligodendrocytes in GLD which may be closely related to the dysfunction and/or degeneration of oligodendrocytes and the demyelination in this disease.
© 2004 Elsevier Inc. All rights reserved.

Keywords: Krabbe disease; Twitcher; Galactocerebrosidase; Oligodendrocyte; Gene therapy; Retrovirus vector

Introduction

Globoid cell leukodystrophy (GLD, Krabbe disease) is a demyelinating disease caused by a genetic deficiency in the activity of a lysosomal enzyme, β-galactocerebros-idase (GALC, EC 3.2.1.46) [1]. In infantile form of this disease, the clinical symptoms occur soon after birth, progress rapidly and most patients die before 2 years of age. The rapid deterioration of the nervous system is postulated to be the result of the dysfunction and/or degeneration of myelin-forming cells (oligodendrocytes

and Schwann cells) caused by an accumulation of galac-tosylsphingosine (psychosine), a cytotoxic metabolite and one of the substrates of GALC [2,3]. To date, there is no effective treatment to this disease except hemato-poietic stem cell transplantation [4].

Twitcher mouse is a naturally occurring genetically authentic murine model of human GLD [5]. Deficiency in the activity of GALC is caused by a nonsense mutation at the coding region of GALC gene [6]. The clinical symptoms of the twitcher mouse include failure to gain weight, tremor, and progressive paralysis of hind limbs and early death around postnatal day 40 (P40). Similar to human GLD, the characteristic pathology in the central and peripheral nervous system (CNS and PNS) of the twitcher mouse is severe demyelination, infiltration

of periodic acid-Schiff (PAS)-positive macrophages, and gliosis. In the brain, oligodendrocytes show morphological alterations and are gradually depleted by apoptotic death [7,8].

The treatments to GLD, like those for most of the other lysosomal storage diseases, are to deliver the deficient enzyme to the cells affected by the storage. Bone marrow transplantation [9–11], neural stem cell transplantation [12], and vector-mediated gene therapy [13,14] in the twitcher mouse showed various degrees of correction of the biochemical, pathological, and clinical phenotypes of the disease. The level of GALC activity appeared responsible for the therapeutic effects. So far, little direct evidence showing that exogenous GALC enzyme was delivered to myelin-forming cells is available. Recent study [15] suggested that down-regulated immune-related molecules in twitcher mouse following bone marrow transplantation may also contribute to clinicopathological improvements. Whether transduction of GALC into myelin-forming cells alone has therapeutic benefit will be crucial in treating GLD, especially by means of gene transfer. In vitro studies showed retrovirus-mediated transduction of GALC led to morphological normalization in cultured oligodendrocytes derived from twitcher mouse [16,17], however taken that the culture system may be different from the in vivo environments such as the absence of immunological environments which is considered to play important roles in the destruction of oligodendrocytes and demyelination in twitcher [18], it is important to clarify whether GALC transduction improves the morphology of the oligodendrocytes in GLD in vivo.

In this study, we introduced human GALC cDNA tagged with myc-epitope into a small number of oligodendrocytes in the twitcher brain by stereotactic injection of retrovirus into the subventricular zone (SVZ) at

birth. By combined immunostaining for the myc-tag and the oligodendroglial specific marker, π form of glutathione-S-transferase (GST-π), we clearly show that GALC transduction led to dramatic morphological improvement of the twitcher oligodendrocytes comparing with those in untreated twitcher controls. The results provided direct evidence that GALC transduction could prevent or correct aberrant morphology of oligodendrocytes in GLD in vivo which may be closely related to the degeneration of oligodendrocytes and the demyelination process in this disease.

Materials and methods

Plasmids

The full-length coding region of human GALC cDNA was cloned [13] and inserted into ClaI site of pBluescript II KS (Stratagene, La Jolla, CA). To assess the influence of ATG surrounding sequence to GALC expression level, the region around the initiation codon was removed using NotI (in +7 position of GALC) and SacI (in the vector), and replaced by three different fragments generated from synthetic complementary oligonucleotides containing an additional ClaI site. The first fragment contains an ATG surrounding sequence initially reported [19,20] and named as "original ATG" in this study. The second fragment contains Kozak consensus sequence [21] named as "Kozak ATG," and the third fragment contains another in-frame ATG at 48 bp upstream to original ATG [22] and named as "1st ATG." The sequences of these fragments were shown in Fig. 1. These three GALC cDNA with different ATG surrounding sequence were excised from pBluescript II KS using ClaI and cloned into ClaI site of retrovirus
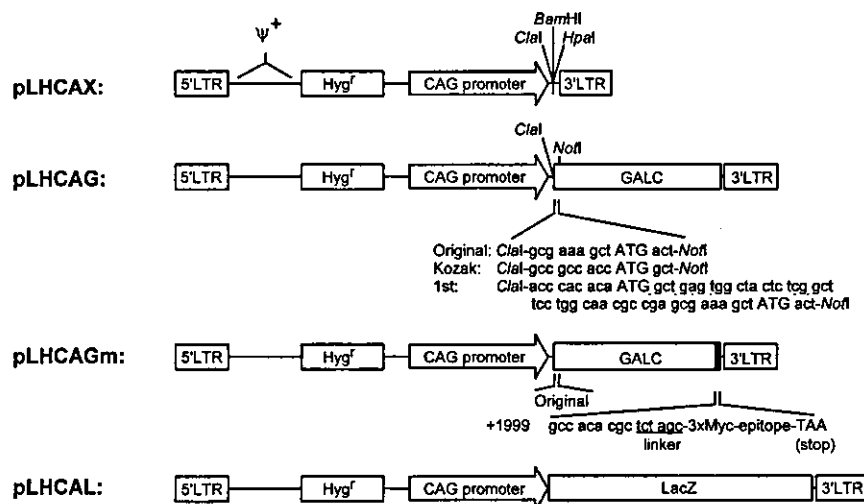

Fig. 1. Schematic representations of the retroviral constructs. See Materials and methods for details.

vector pLHCAX [23] to generate a series of retroviral vectors named pLHCAG (Fig. 1). In which, a hygromycin phosphotransferase gene was driven by the long terminal repeat (LTR) and GALC gene was driven by CAG promoter. To introduce myc-epitope, the stop codon (TAA, in +2008 position) of GALC (with "original ATG") was replaced with a unique XbaI site by polymerase chain reaction (PCR)-based mutagenesis. Complementary oligonucleotides encoding three tandem c-myc-epitope (EQKLISEEDL) followed by a stop codon (TAA) was cloned in-frame into XbaI site to create pLHCAGm (Fig. 1). In all ligated plasmids, the orientation and sequence of each insert was confirmed by DNA sequencing. A retrovirus vector expressing Escherichia coli β-galactosidase (β-gal), pLHCAL [23], generated by the insertion of LacZ gene between the BamHI and HpaI sites of pLHCAX was also used in this study (Fig. 1).

Transient expression study

Bosc23 and NIH/3T3 cells were grown in 12-well plates (NunC, Roskilde, Denmark) at 37°C with 5% CO_2 in Dulbecco's modified Eagle's medium (DMEM) with high glucose (4.5 g/L) supplemented with 10% (v/v) heat-inactivated fetal bovine serum (FBS). When approximately 95% confluent, the cells were transfected using Lipofectamine 2000 reagent (Invitrogen, Carlsbad, CA) according to the manufacturer's recommendation (1.6 μg DNA:4 μl lipofectamine 2000 per well). Two days after transfection, the cells were washed with phosphate-buffered saline (PBS), harvested and assayed for GALC activity (as described below).

Virus preparation

To produce recombinant retrovirus, ecotropic packaging cell line ψMP34 [24] was transfected by calcium phosphate method (Cellphect transfection kit, Amersham, Piscataway, NJ) with pLHCAGm. After selection with 0.5 mg/ml hygromycin B (Wako, Osaka, Japan), drug-resistant colonies were isolated and a subclone (ψMP34/pLHCAGm#92) producing the highest titer of LHCAGm was used in this study. Retrovirus was concentrated according to the protocol reported by Bowles et al. [25] as described previously [23].

Viral titer assay and in vitro infection

For the assessment of infectious viral titers, NIH/3T3 target cells were grown in 24-well plates (for LHCAGm) or 6 cm dishes (for LHCAL) in DMEM supplemented with 10% FBS. When approximately 60% confluent, cells were infected with serially diluted viral stocks overnight at 37°C in the presence of 8 μg/ml polybrene (Sigma, St. Louis, MO). Forty-eight hours after infection, cells were

fixed and stained to detect transgene expressing cells. The cells infected with LHCAGm were fixed with 4% paraformaldehyde in PBS for 10 min on ice, and stained for myc-epitope using rabbit polyclonal antibody to myc-tag (MBL, Nagoya, Japan, 1:1500) as described in histochemical analysis section below. The cells infected with LHCAL were fixed with 0.25% glutaraldehyde in PBS and stained with X-gal solution (1 mg/ml X-gal, 5 mM potassium ferricyanide, 5 mM potassium ferrocyanide, and 2 mM $MgCl_2$ in PBS) overnight at 37°C. The number of positively stained colonies was counted under a microscope and the titer was calculated as follow: cfu/ml = number of positive colonies/virus volume (ml). The titers of concentrated LHCAGm and LHCAL were 1.2×10^7 and 7.3×10^7 cfu/ml, respectively.

To evaluate intracellular activity of transduced GALC gene, spontaneously immortalized fibroblasts derived from twitcher mouse designated as Tw2 were infected with LHCAGm in the presence of 8 μg/ml polybrene and selected with 0.5 mg/ml hygromycin B. A drug-resistant subclone (Tw2/LHCAGm#11) with the highest GALC activity was expanded and used for the galactocerebroside (GalCer)-loading study.

Animals and virus injection

Breeding pairs of twitcher heterozygotes (C57BL/6J, twi/+) were purchased from the Jackson Laboratory (Bar Harbor, ME) and maintained in our laboratory under standard housing condition. To determine transduction pattern of SVZ injection in the mouse, nine normal C57BL/6J mice received LHCAL injection at P0 were analyzed for gene transfer to the neural cells by X-gal staining (at P4) or immunohistochemistry for β-gal (at P30). Twenty twitcher mice were used in this study: 10 mice received LHCAGm injection and seven out of eight surviving recipients were used for histochemical (n = 4) or biochemical (n = 3) analysis at P35–40; three received LHCAL injection and used for histochemical analysis at P38–39 and seven untreated twitcher mice were taken as controls for histochemical (n = 4) or biochemical (n = 3) analysis at P39–40. In addition, six untreated normal mice were used as controls for histochemical (n = 3) or biochemical (n = 3) analysis at P40.

The procedure of stereotactic injection of retrovirus into SVZ was modified from that reported by previous study in neonatal rats [26]. Briefly, the injection was performed on the day of birth after DNA diagnosis of the twitcher mutation by PCR [6]. The newborn mice were anesthetized by placing on ice for a few minutes, placed in a stereotactic apparatus (Narishige, Tokyo, Japan) and kept cold with ice packs. Approximately 1.0 μl HBSS containing retrovirus with 0.01% Fast Green (Sigma) was injected unilaterally through a 30 G needle with a micro syringe (Ito, Shizuoka, Japan). Stereotactic

coordinates (related to the intersection of transverse and longitudinal cerebral fissure) were anterior 1.5 mm and lateral 1.5 mm, at a depth of 2 mm. All pups used in this study were recovered from cryoanesthetization by warming prior to being returned to their mother.

The Fast Green dye was used to verify that the virus was not injected into the lateral ventricle. In pilot studies using LHCAL in normal mice showed that when retrovirus was injected into the cerebral ventricles few cells could be transduced in any location of the brain. In one twitcher mouse received LHCAGm injection in this study, virus entered the lateral ventricle and few myc$^+$ cell was found in the brain and no further analysis was carried out on this animal.

GALC activity assay

GALC activity was assayed as previously described [27] using ^{3}H-labeled GalCer as substrate. The cells were washed with PBS, harvested, and sonicated for 30 s on ice. For tissues, the forebrain was homogenized in distilled water with Potter–Elvehjem homogenizer and sonicated briefly. The homogenate corresponding to about 100 μg of total proteins was used for the assay. Protein concentrations were determined with BCA protein assay reagent (Pierce, Rockford, IL) with bovine albumin as standard.

Galactocerebroside-loading study

Galactocerebroside (GalCer)-loading study was performed essentially as described by Kobayashi et al. [28,29]. Briefly, ^{3}H-labeled GalCer in chloroform:methanol (2:1, v/v) and phosphatidylserine in chloroform:methanol (95:5, Sigma) were dried in a sterilized tube and mixed with DMEM supplemented with 10% FBS by sonication for 30 min. Confluent Tw2, Tw2/LHCAGm#11, and NIH/3T3 cells grown in 3.5 cm dishes were incubated with 1.5 ml the medium containing 0.33 μg [^{3}H]GalCer (12,000 dpm)/ml and 5 μg phosphatidylserine/ml. After 4 days, the medium was removed and cells were harvested by trypsin digestion. Intracellular [^{3}H]GalCer and released [^{3}H]galactose in medium was extracted as described [29], dissolved in ACSII scintillation cocktail (Amersham) and the radioactivities were counted in a scintillation counter (LS6500, Beckman Instruments, Fullerton, CA). Hydrolysis of GalCer was expressed as a percentage of the released galactose, on the basis of the total incorporated GalCer (the sum of galactose in the medium and intracellularly accumulated GalCer).

Western blot

The confluent cells grown in 6 cm dishes were lysed with 300 μl sample buffer. After heating at 95 °C for 5 min, 5 μl of total cell lysates were electrophoresed on a

10% sodium dodecylsulfate (SDS)–polyacrylamide gel and blotted to a PVDF membrane (Novex, San Diego, CA). The membrane was reacted with rabbit polyclonal antibody to myc-tag (MBL, 1:1000) at 4 °C overnight and the signals of reactive proteins were detected by ECL plus reagents (Amersham).

PCR and Southern blot

Total cellular RNA was extracted from the brain homogenate of the recipients and untreated control mice using RNeasy lipid tissue kit (Qiagen, Hilden, Germany) following the manufacturer's instructions including DNase I treatment. The reverse-transcription reaction was performed using the SuperScript first-strand synthesis system (Invitrogen) with oligo(dT) primer. Genomic DNA was extracted from brain homogenate from treated twitcher mice and untreated control mice by DNeasy tissue kit (Qiagen). The primers specific for human GALC cDNA were designed as 5'-TGGAA CCCATTCAG<u>CAAAAG</u>-3' (forward primer) and 5'-CTGCTTAAAAAGAAATCTTT<u>CGGAT</u>-3' (reverse primer, amplicon length of 559 bp). The forward and reverse primer located in exons 8 and 12, respectively, spanning more than 17 kb of introns in genome, and the last 5–6 nucleotides (underlined) in 3'-termini are completely different from the sequences of the mouse GALC cDNA. Genomic DNA (100 ng) or cDNA corresponding to 0.6 μg total RNA were added to AmpliTaq Gold Master Mix (ABI, Tokyo, Japan) containing 0.5 μM of each primer in a final volume of 50 μl. The PCR was carried out as denaturation at 95 °C for 5 min, followed by 30 cycles of denaturation at 95 °C for 15 s, annealing at 55 °C for 15 s and extension at 72 °C for 1 min. Under these conditions, no amplification occurs in mouse genomic DNA or cDNA.

Ten microliters of PCR products were electrophoresed on a 1.5% agarose gel, photographed after ethidium bromide staining and transferred to a nylon membrane. The membrane was hybridized with a [^{32}P]dCTP labeled human GALC probe (1.1 kb *Hind*III–*Sph*I fragment of GALC cDNA) and exposed to X-ray film (Fuji Photo Film, Tokyo, Japan).

Histochemical analysis

The mice were anesthetized and fixed with transcardial perfusion of chilled 4% paraformaldehyde in 0.1 M phosphate buffer (PB, pH 7.4) at the time of analysis. Brains were removed and postfixed in the same fixative overnight at 4 °C and cryoprotected in 15% sucrose in 0.1 M PB. Consecutive coronal sections of the forebrain were made at a thickness of 20 μm using a cryostat.

For immunohistochemistry, the sections were incubated with 0.3% Triton X-100 in 0.1 M PBS (PBST) for overnight at 4 °C, then treated with 0.5% H_2O_2 in PBST

for 30 min at room temperature (RT) to eliminate endogenous peroxidase activity. After incubation with 5% normal goat serum (NGS) in PBST for 1 h at RT, the sections were incubated with primary antibody (rabbit anti-β-gal, 5' → 3', Boulder, CO, 1:500; rabbit anti-myc-tag, MBL, 1:500 or rabbit anti-GST-π, MBL, 1:20,000) diluted in 3% NGS/PBST for overnight at 4 °C. The sections were then incubated with biotinylated goat anti-rabbit IgG (Vector Laboratories, Burlingame, CA) diluted 1:200 in 3% NGS/PBST for 1 h at RT, followed by the incubation for 30 min with avidin–biotin complex (ABC) reagent (ABC elite kit; Vector Laboratories) at RT. The peroxidase labeling was visualized with 3,3'-diaminobenzidine (DAB) substrate (Vector Laboratories) with or without nickel chloride.

For double immunostaining, after treated with Triton X-100 and H_2O_2 as above the sections were incubated in order with blocking reagents, primary antibody (mouse monoclonal anti-β-gal, Promega, Madison, WI; 1:1000 or mouse monoclonal anti-myc (9E10), Santa Cruz Biotechnology, Santa Cruz, CA, 1:1000), biotinylated anti-mouse IgG reagent and ABC reagent (Vector MOM peroxidase kit, Vector Laboratories) according to kit instructions except for incubation with primary antibody overnight at 4 °C. The 3-amino-9-ethylcarbazole (AEC, Sigma) was used to localize peroxidase and the sections were kept in PBS on ice. The immunoreactive cells in the cerebral cortex were viewed and photographed under light microscope (4× and 40× objective) connected with a color CCD camera (Olympus, Tokyo, Japan) to document the positions and morphologies of positive cells. Then sections were immersed in a graded ethanol series to eliminate AEC reaction product. After rehydrated and treated with 0.5% H_2O_2 to eliminate any residual peroxidase activity, the sections were incubated with rabbit polyclonal antibody to GST-π (MBL, 1:8000) for 5 days at 4 °C and labeled with ABC elite kit (Vector Laboratories) as described above, visualizing peroxidase with DAB-nickel (Vector Laboratories). The sections were dehydrated, cleared, and mounted.

The AEC reaction product was eliminated before the second immunostaining because cytoplasmic localization of β-gal or myc tagged GALC was largely overlapped with that of the second antigen GST-π and the dense AEC product appeared interfere with subsequent processes of immunostaining to detect GST-π. However, based on carefully documented anatomical locations including relation with nearest vessels and the morphologies of positive cells after immunostaining of the first antigen, the majority of doubly positive cells were easily identified after GST-π immunostaining (see Figs. 6G–J). Every third section at the levels corresponding to level 15–25 in the "Brain Maps: Structure of the Rat Brain" by Swanson [30] were used for morphological analysis of GST-π⁺ cells and for untreated controls one section per

animal at level 25 was used for the analysis. The morphology of the cells after GST-π staining was examined under microscope and photographed.

Immunofluorescence study

Tissues were prepared as described above and double immunofluorescence was performed as previously described [13]. The used primary antibodies were: mouse monoclonal anti-β-gal (Promega, 1:500), rabbit polyclonal anti-glial fibrillary acidic protein (GFAP; Dako, Glostrup, Denmark; 1:300), rabbit polyclonal anti-GST-π (MBL, 1:500) and rabbit polyclonal anti-myelin basic protein (MBP; Dako; 1:500). The secondary antibodies used were: rhodamine-conjugated goat anti-mouse IgG and FITC-conjugated goat anti-rabbit IgG (Cappel, Aurora, OH; 1:100). The sections were viewed under a fluorescence microscope and photographed using an AquaCosmos CCD camera (Hamamatsu Photonics, Hamamatsu, Japan).

Results

Determination of influence of ATG surrounding sequence to GALC activity

It is known that the sequence around the initiation codon in GALC gene is not optimal for translation according to Kozak rule [19–21]. Prior to the generation of recombinant retrovirus, to determine the sequence around initiation codon that gives rise to the most optimal expression of GALC, we generated three expression vectors carrying GALC cDNA with "original ATG," "Kozak ATG" and "1st ATG," respectively (Fig. 1). Transient expression studies ($n = 6$) in Bosc23, a cell line derived from the kidney of human embryo, showed no significant difference in GALC expression level among these three constructs. When expression study was performed in NIH/3T3 cells ($n = 3$), expression level from "original ATG" was higher than that of "Kozak ATG" or "1st ATG" with statistically significant difference (Fig. 2). The results indicate that pLHCAG (original) has comparable or better expression level than the other two constructs. And GALC gene with "original ATG" was used in subsequent study.

Epitope tagging of GALC gene

To favor the convenient identification of cells expressing transduced GALC gene in tissues, c-myc-epitope (1 or 3 copies) was introduced to the carboxyl-terminus of GALC with the "original ATG." In a pilot study, immunofluorescence against myc-tag after transfection showed that tandem three copies of the tag significantly improved signal strength comparing with a single copy
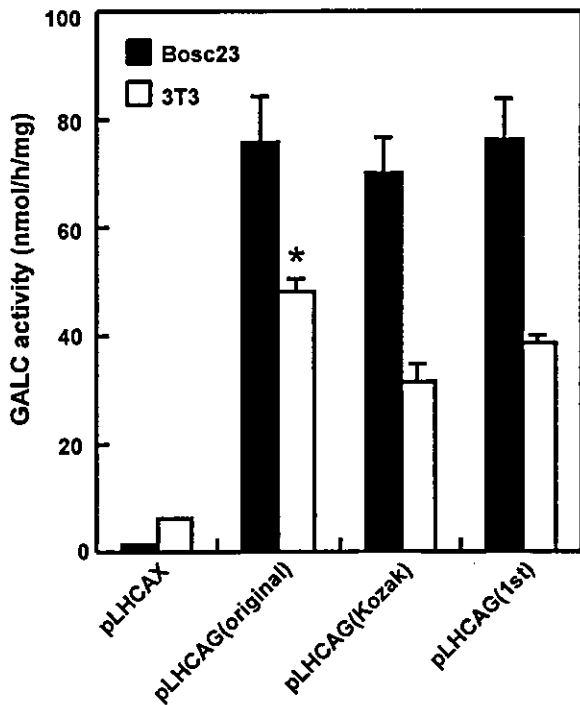
Fig. 2. Influence of ATG surrounding sequence to GALC activity. GALC activities in Bosc23 (n = 6) and NIH/3T3 (n = 3) cells transfected with retroviral vectors carrying GALC cDNA with "original ATG", "Kozak ATG" or "1st ATG." pLHCAX was used as control vector. The data are presented as mean ± SE *P = 0.015 and 0.038, ("original ATG" compared with "Kozak ATG" and "1st ATG" respectively, t test).

Fig. 3. Characterization of epitope tagged GALC protein. (A) GALC activities in Bosc23 (n = 3) transfected with retroviral vectors carrying GALC with (pLHCAGm) or without myc-tag (pLHCAG). pLHCAX was used as control vector. The data are presented as mean ± SE. (B) Hydrolysis rates of GalCer in twitcher fibroblasts (Tw2), a subclone of retrovirus LHCAGm-infected Tw2 (Tw2/LHCAGm#11) and NIH/3T3, assessed by [³H]GalCer loading test (n = 2). (C) Myc-tag-immunocytochemistry in a subclone of ψMP34 stably transduced with pLHCAGm (ψMP34/pLHCAGm#92). Parental ψMP34 is a mouse fibroblasts-derived packaging cell line. (D) Western blot analysis of cell extracts from parental cell line ψMP34 (lane 1) and two subclones of ψMP34 stably transduced with pLHCAGm (ψMP34/pLHCAGm#92 and #96; lanes 2 and 3, respectively) labeled with rabbit antibody to the myc-tag. The molecular weight standards are shown on the left. Transgene-specific bands are indicated by arrowheads.

of tag, so the construct encoding GALC with triple epitope-tag (named as pLHCAGm, Fig. 1) was used subsequently to produce recombinant retrovirus.

It is critical to determine whether epitope-tag interferes with the normal structure and biological activity of GALC protein. Transient expression study showed that no decrement of GALC activity in the cells transfected with pLHCAGm comparing with the parent construct without epitope tagging (Fig. 3A). To further confirm that epitope tagging has no adverse effects on GALC, [³H]GalCer loading test was carried out on a subclone of twitcher fibroblasts expressing myc-tagged-GALC (Tw2/LHCAGm#11;GALC activity: 14.07 nmol/h/mg). The hydrolysis rate of GalCer in Tw2/LHCAGm#11 significantly increased as compared with uninfected parental twitcher fibroblasts (Tw2), near that in NIH/3T3 cells (Fig. 3B). This demonstrated that GALC deficiency in the twitcher cells was restored by LHCAGm transduction and that epitope tagging has no influence on lysosomal targeting and intracellular catalytic activity of recombinant GALC protein.

Immunocytochemistry using antibody against myc-tag in cells stably transduced with pLHCAGm showed punctated stains throughout the cytoplasm (Fig. 3C). Western blot analysis of cell extracts from these cells
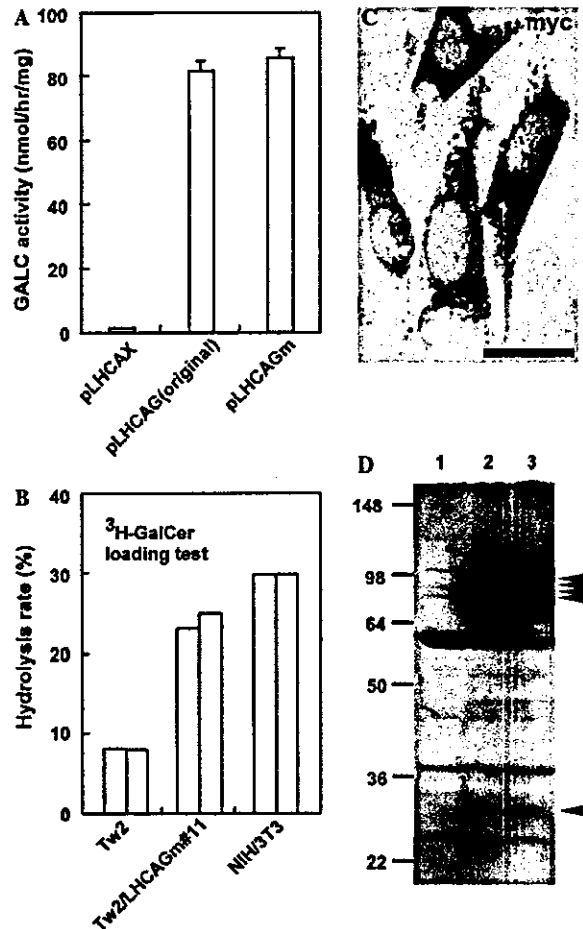
showed transgene-specific bands between 80 and 90 kDa (four bands could be identified in shorter time of exposure) and one at about 30 kDa (Fig. 3D, arrowheads). The bands of 80–90 kDa may present the precursor form of GALC and the band near 30 kDa may present the C-terminal subunit of GALC [31–33]. The signal strength in 80–90 kDa was significantly stronger than that in 30 kDa suggesting that most of the immunoreactive signals observed in the immunocytochemical study above may be contributed to the precursor form of GALC protein.

Stable gene transfer to oligodendrocytes by SVZ injection of retrovirus

To transduce oligodendrocytes in vivo, we introduced retrovirus into the SVZ at neonatal period in the mouse. To investigate the pattern of gene transfer by SVZ injection, LHCAL was injected stereotactically into the SVZ of neonatal normal mice and the transduction pattern was examined by X-gal histochemistry and immunohistochemistry at P4 and P30. No noticeable inflammatory and other abnormality was observed in the brain. At P4, many β-gal$^+$ cells still remained in the SVZ and some positive cells were observed in the cortex and the white matter dorsal or lateral to the SVZ (Fig. 4A). At P30, when migration and differentiation of neural cells are almost completed in the mouse brain, β-gal$^+$ cells were scattered widely in the neocortex, subcortical white matter, and the striatum of the ipsilateral hemisphere (Fig. 4B). Few positive cells could be seen in the contralateral hemisphere. All transduced cells appeared to be glia and most of them could be classified into oligodendrocytes and astrocytes by morphological criteria described previously [26]. No β-gal$^+$ neuron could be found. Transduced oligodendrocytes were distributed both in the gray and white matter. In the white matter β-gal$^+$ oligodendrocytes had many longitudinal processes parallel to nerve fiber tract presumably the cytoplasmic tongues of myelin sheaths (Fig. 4C), while many transduced oligodendrocytes in the cerebral cortex showed abundant, tenuous processes corresponding to type I oligodendrocytes [34] (Fig. 4D). Most transduced astrocytes have protoplasmic morphology with highly branched feather-like processes (Fig. 4E). Cell type identification was further confirmed by double immunofluorescence using antibodies to both β-gal and cell type-specific markers (GFAP for astrocytes, GST-π and MBP for oligodendrocytes) (Figs. 4F and G).

The results were essentially consistent with earlier studies in rats [26] and demonstrated that SVZ injection of retrovirus in neonatal mouse is an ideal strategy to achieve persistent transduction of oligodendrocytes from early developmental stages.

Transduction of GALC to twitcher brain

GALC-expressing retrovirus LHCAGm was injected into the SVZ of twitcher mice at P0. Two out of 10 recipients disappeared at the next day and eight recipients survived at the time of analysis. No changes in the clinical symptoms such as small body, twitching and paralysis of hind limbs were observed in the LHCAGm injected twitcher mice comparing with untreated twitcher controls.

At P38–40, LHCAGm injected twitcher brains were studied for transgene expressing-cells by immunohistochemistry against myc-tag. Myc$^+$ cells were identified in
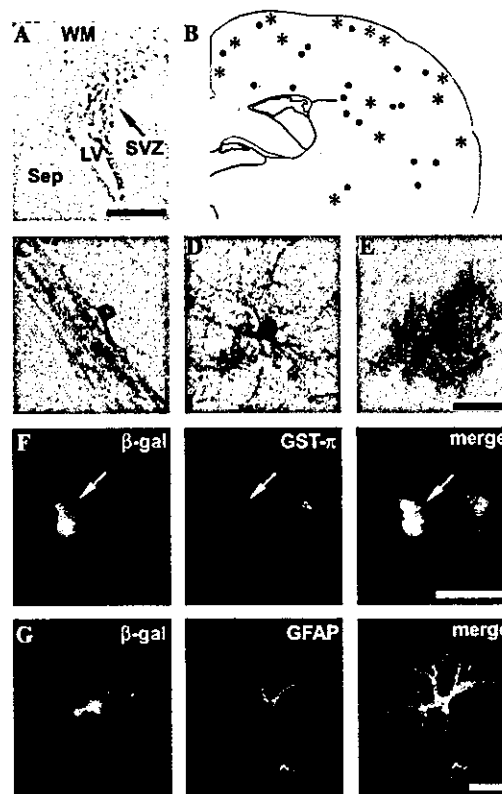

Fig. 4. Gene transfer to the brain of normal mouse by SVZ injection of LHCAL. (A) X-gal stained coronal brain section at P4 shows many β-gal$^+$ cells (blue) located in the SVZ. The level of the section nears the site of injection. (B) Schematic representation of the distribution of β-gal$^+$ cells based on immunostaining to β-gal in the recipient's brain at P30. Closed circles and asterisks represent positive oligodendrocytes and astrocytes respectively. (C–E) Microscopic photographs of β-gal-immunoreactive glial cells in the recipients brain at P30. (C) A positive oligodendrocyte in the white matter. Note immunoreactive longitudinal processes parallel to the nerve tract. (D) An immunoreactive oligodendrocyte in the cerebral cortex. (E) A positive protoplasmic astrocyte in the cerebral cortex. (F and G) Cell-type identification of transduced cells by double immunofluorescence. (F) A β-gal-immunoreactive cell (red) in the cerebral cortex was GST-π$^+$ (green), indicating it is an oligodendrocyte. (G) Two β-gal-immunoreactive cells (red) in the cerebral cortex were GFAP$^+$ (green), indicating they are astrocytes. The two cells contact closely suggesting they may be daughters of the same progenitor. LV, lateral ventricle; WM, white matter; Sep, septum; SVZ, subventricular zone. The schema of the brain in (B) was adopted from "Brain Maps: Structure of the rat Brain" by Swanson [30]. Scale bar: 250 μm in (A); 25 μm in (C–E); 20 μm in (F and G). (For interpretation of the references to colors in this figure legend, the reader is referred to the web version of this paper.)

four out of five examined twitcher brains. The distribution pattern of myc$^+$ cells in the brain sections was similar to that of β-gal$^+$ cells observed in the LHCAL injected normal mice described above. The number of myc$^+$ cells in the twitcher brain varies slightly among animals with an average number of ~10 cells in the cerebral cortex per section. All myc$^+$ cells were glial cells and most of them could be defined as either oligodendrocytes or astrocytes by their morphology. The transduced

oligodendrocytes exhibited an intense cytoplasmic stain-
ing with moderately stained asymmetrical nucleus (Fig.
6E). Only a few proximal processes extended from cell
body could be identified in LHCAGm transduced oligo-
dendrocytes. Myc⁺ astrocytes exhibited stains in the rim
of cytoplasm and abundant bushy processes with rela-
tively pale nucleus (Fig. 6F).

The presence and expression of transduced GALC
gene in the recipient twitcher brain was analyzed by
PCR and RT-PCR using primers specific for human
GALC at P35–39 (Fig. 5). All three twitcher recipients'
brains examined were positive for human GALC cDNA
(provirus DNA) and human GALC transcript. The
authenticity of the PCR product was confirmed by
Southern blot with a human GALC probe. GALC
expression was further assessed by enzymatic assay.
There was no measurable GALC activities in the trans-
duced twitcher brain above untreated twitcher controls
(GALC activities: 0.05 ± 0.01, 0.08 ± 0.01, and 2.24 ±
0.14 nmol/h/mg in transduced twitcher, age-matched
untreated twitcher and untreated normal mouse brain,
respectively, each three animals). This was not unex-
pected since the number of transduced cells in the brain
was very small. The activity of transduced GALC in the

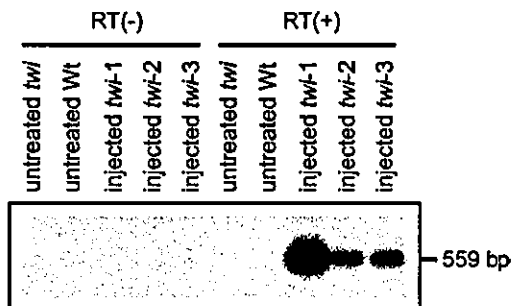**A Provirus DNA**

— 559 bp

B mRNA expression

— 559 bp
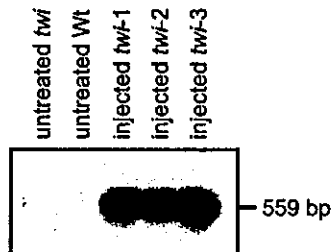
Fig. 5. Presence and expression of transduced human GALC in the
twitcher brains which received neonatal SVZ injection of LHCAGm.
Southern blot analysis. (A) PCR amplification of genomic DNA from
the whole brain to detect the presence of the integrated provirus. (B)
Human GALC transcript was detected by RT-PCR using total RNA
from the whole brain. The authenticity of PCR products was con-
firmed by hybridized with a human GALC probe. RT(+) and RT(−)
indicate amplified PCR products form cDNA samples with and with-
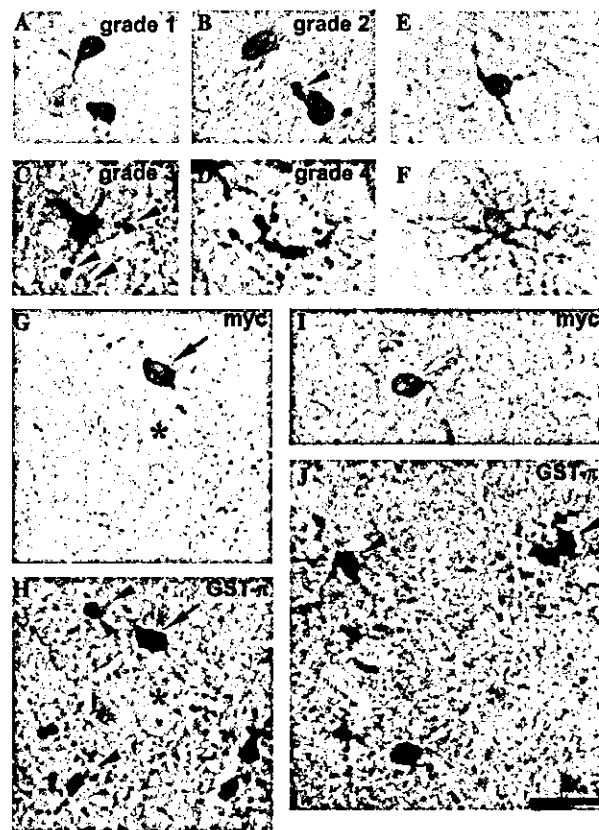out reverse transcriptase, respectively.

Fig. 6. Morphological correction of twitcher oligodendrocytes by
GALC transduction. (A–D) The severity of morphological aberra-
tions of oligodendrocytes in the cerebral cortex was divided into four
grades by GST-π-immunostaining. (E and F) LHCAGm transduced
oligodendrocyte (E) and astrocyte (F) in the twitcher cerebral cortex at
around P40, identified by immunohistochemistry against myc-tag. (G
and H) A representative brain section from LHCAGm injected
twitcher cerebral cortex subsequently stained with mouse anti-myc-tag
(G, chromogen: AEC) and rabbit anti-GST-π (H, chromogen: DAB-
NiCl₂) antibodies. A myc⁺/GST-π⁺ cell (arrow) exhibits normal mor-
phology (Grade 1), while myc⁻/GST-π⁺ cells (arrowheads) show
severe aberrant morphologies (Grades 3 and 4). Asterisk indicates the
blood vessel nearing myc⁺ cell as anatomic marker. (I and J) Another
brain section stained with anti-myc (I) and anti-GST-π (J) antibodies.
Scale bar: 20 μm.

whole brain homogenate may be under the detection
limit of this enzyme assay system.

*Morphological improvements in GALC transduced
oligodendrocytes in the twitcher brain*

To evaluate the effects of GALC transduction on the
morphology of oligodendrocytes, an analysis using
combined immunostaining for myc-epitope and GST-π
was carried out. GST-π has been well documented as a
marker of oligodendrocytes [35] and previously used to
investigate morphological aberrations in twitcher
oligodendrocytes [8]. Unlike many other oligodendrog-
lial markers such as MBP, 2′,3′-cyclic nucleotide